

# Fluctuations and Correlations in Causal Set Theory

---

Heidar Moradi,<sup>a</sup> Yasaman K. Yazdi<sup>b,c</sup> and Miguel Zilhão<sup>d</sup>

<sup>a</sup>*Physics and Astronomy, Division of Natural Sciences, University of Kent, Canterbury CT2 7NZ, United Kingdom*

<sup>b</sup>*School of Theoretical Physics, Dublin Institute for Advanced Studies, 10 Burlington Road, Dublin 4, Ireland.*

<sup>c</sup>*Theoretical Physics Group, Blackett Laboratory, Imperial College London, SW7 2AZ, United Kingdom*

<sup>d</sup>*Centre for Research and Development in Mathematics and Applications (CIDMA), Department of Mathematics, University of Aveiro, 3810-193 Aveiro, Portugal*

*E-mail:* [h.moradi@kent.ac.uk](mailto:h.moradi@kent.ac.uk), [ykyazdi@stp.dias.ie](mailto:ykyazdi@stp.dias.ie), [mzilhao@ua.pt](mailto:mzilhao@ua.pt)

**ABSTRACT:** We study the statistical fluctuations (such as the variance) of causal set quantities, with particular focus on the causal set action. To facilitate calculating such fluctuations, we develop tools to account for correlations between causal intervals with different cardinalities. We present a convenient decomposition of the fluctuations of the causal set action into contributions that depend on different kinds of correlations. This decomposition can be used in causal sets approximated by any spacetime manifold  $\mathcal{M}$ . Our work paves the way for investigating a number of interesting discreteness effects, such as certain aspects of the Everpresent  $\Lambda$  cosmological model.

---

## Contents

<b>1</b>	<b>Introduction</b>	<b>2</b>
<b>2</b>	<b>Causal Sets and Poisson Sprinkling</b>	<b>4</b>
2.1	Causal Set Theory	4
2.2	Poisson Sprinkling	5
<b>3</b>	<b>Correlations Between Quantities in Different Regions</b>	<b>7</b>
3.1	The $\zeta$ -function (Cardinality Indicator)	7
3.1.1	General Properties of $\zeta$	8
3.2	The $\chi$ -function (Occupation Indicator)	10
3.3	Correlation Functions	11
3.3.1	Example Calculations	13
3.3.2	Careful Treatment of $\zeta - \chi$ Correlations	15
<b>4</b>	<b>Causal Set Action</b>	<b>16</b>
<b>5</b>	<b>Fluctuations of the Causal Set Action</b>	<b>18</b>
5.1	Integral Formulation	19
5.2	Special Case $\mathcal{K}_{-1,j}$	21
5.2.1	$\mathcal{K}_{-1,-1}$	21
5.2.2	$\mathcal{K}_{-1,j}$	21
5.3	General Case $\mathcal{K}_{ij}$	22
5.3.1	$\chi$ - $\chi$ Correlations	23
5.3.2	$\zeta$ - $\chi$ Correlations	24
5.3.3	The $J^1$ Integral	25
5.3.4	The $J^4$ Integral	25
5.3.5	The $J^2$ Integral	26
5.3.6	The $J^6$ Integral	27
5.4	Core Set of Integrals	27
<b>6</b>	<b>Conclusions and Outlook</b>	<b>29</b>
<b>A</b>	<b>Expressions for Correlation Functions</b>	<b>30</b>
<b>B</b>	<b>Products of <math>\chi</math> Functions</b>	<b>31</b>
<b>C</b>	<b>Parametrization of Integration Domains</b>	<b>33</b>
C.1	Example: Parametrization of $\mathcal{J}^-(x_1) \cap \mathcal{J}^-(x_2)$ in a 1+1D Minkowski Diamond	33
C.2	Example: Parametrization of $\mathcal{J}^-(x)$ in a 3 + 1D Minkowski Diamond	34

---

## 1 Introduction

Causal set theory proposes that spacetime is fundamentally discrete and the causal relations among the discrete elements play a prominent role in the physics [1, 2]. Fundamental discreteness of spacetime is a promising idea for understanding the finiteness of black hole entropy [3] and resolving the UV divergences of quantum field theories and spacetime singularities. Discreteness is also known to avoid other subtleties such as quantum anomalies [4–8]. A causal set is made up of elements of spacetime, presumed to be roughly a minimum Planck distance apart, with nothing in between them. This stark difference with continuum spacetime requires us to rethink how familiar smooth quantities can emerge. It also offers new possibilities to probe unknown physics as well as currently unexplained phenomena.

Progress has been made in recognizing and understanding how some continuumlike features can emerge from causal sets at macroscopic scales, i.e., when the number of elements is large. An important result in this direction is that a causal set is well approximated by a continuum spacetime if there is a number-volume correspondence between the causal set and spacetime. This occurs when the number of elements  $N$  within an arbitrary spacetime region with spacetime volume  $V$  is statistically proportional to  $V$  [9]. Such a correspondence is not guaranteed to exist for any causal set, and in fact it does not exist for a large class of causal sets which are said to be *non-manifoldlike* (see e.g. [10, 11]). On the other hand, such a correspondence is guaranteed (with minimal variance [9]) when the number of causal set elements is randomly distributed according to the Poisson distribution. The proportionality constant between the mean number  $\langle N \rangle$  and volume  $V$  is the discreteness scale  $\rho$ , namely  $\langle N \rangle = \rho V$ , and the standard deviation  $\Delta N = \sqrt{\rho V}$  according to the Poisson distribution. The number-volume correspondence makes it possible to compare discrete quantities with continuum quantities, and the Poisson distribution and the statistics it induces are at the heart of this subject.

As alluded to above, the number-volume correspondence is not exact. There are statistical fluctuations away from the mean. For small deviations from the mean, these fluctuations can be regarded as corrections to continuum geometric quantities and their functions. At the very least, these fluctuations are discrete but still classical corrections. There are also, however, hints as to how such discreteness and fluctuations may relate to and affect quantum phenomena. For example, fundamental discreteness of the kind inherent in causal sets has led to new<sup>1</sup> and UV regular formulations of quantum field theory [12–14] and entropy [15–17] on a background causal set. This includes a class of nonlocal d’Alembertians [18, 19]. There is evidence that the means of these d’Alembertians in causal sets approximated by curved spacetimes agree with the usual continuum d’Alembertian *plus* a term approximated by the Ricci scalar curvature and certain boundary terms. The latter term has been used to define a causal set analogue of the Einstein-Hilbert gravitational action [19].

In a different context and in much earlier work, a cosmological model known as Everpresent  $\Lambda$  [20–24] was introduced whose crucial ingredient is the statistical deviation from

---

<sup>1</sup>These quantum field theories are defined with respect to spacetime rather than spatial foliations.

the number-volume correspondence. Everpresent  $\Lambda$  is a model for a fluctuating cosmological constant which is a direct consequence of the standard deviation of the Poisson distribution and a quantum uncertainty relation between  $\Lambda$  and the spacetime volume. It further takes the quantum uncertainty in  $V$  to be the statistical fluctuation in  $V$  due to discreteness, thereby implicitly linking the Poisson distribution of the number-volume correspondence to a quantum origin. The model correctly predicts the value of the cosmological constant today and is a candidate solution to current cosmological tensions [25–27], making its study especially timely. In this model the value of the cosmological constant fluctuates over cosmic history, but the precise correlation timescale and dynamics governing these fluctuations is not yet known. The dynamical nature of dark energy in models of Everpresent  $\Lambda$  make it especially promising as a candidate solution to the Hubble tension [28]. The recent DESI [29] observations also favor dynamical dark energy models.

The causal set action mentioned earlier, defined using the nonlocal and discrete d’Alembertian, also has fluctuations about the mean value. A natural and interesting question is: could there be an Everpresent  $\Lambda$  term in the fluctuations of the causal set action? In other words, could the fluctuations of the causal set action be the source of Everpresent  $\Lambda$ ? It is also natural to expect there to be a connection between the discrete gravitational action and the cosmological constant, in close analogy with a cosmological constant term often appearing in the continuum gravitational action. While the scope of our work is wider than applications to the causal set action, our focus will be the fluctuations of the action as it paves the way for studying this question. There are several open questions regarding Everpresent  $\Lambda$ <sup>2</sup> which we would be in a better position to answer if the fluctuations of the action could be used to model it. There are currently two phenomenological models of Everpresent  $\Lambda$  (known as Model 1 and Model 2) in the literature. If the causal set action can be used to model Everpresent  $\Lambda$ , it would provide a third phenomenological model that is independent of Models 1 and 2. Moreover, there are important avenues of investigation for building a path integral dynamics of causal sets. Knowledge of the fluctuations of the action would facilitate a more thorough study of these dynamical models as well as their stability characteristics. When we consider the path sum or partition function  $\sum_{\mathcal{C}} e^{iS(\mathcal{C})}$ , the action that we use will ultimately not be an averaged one, and hence the higher statistics such as the standard deviation will play a role.

The broad aim of this paper is to formalize the approach to studying and calculating fluctuations within causal set theory. Another major aim of this paper is to provide a comprehensive discussion on the topic of correlations within causal set theory. An example of a correlation would be: the correlation between the probability of the past lightcone

---

<sup>2</sup>One such open question is how to determine the mean about which fluctuations occur. In current models, the mean is assumed to be 0, but this choice still needs to be motivated. Another open question is how to incorporate spatial inhomogeneities, which are needed in any realistic cosmological model in order to explain structure formation. Current models of Everpresent  $\Lambda$  only incorporate temporal inhomogeneities. Yet another important open question, which was already briefly mentioned, is what the dynamics governing the fluctuations of  $\Lambda$  are and how the fluctuations at different epochs correlate with one another. At present, slightly modified versions of the Friedmann equation(s) are used, but a better understanding of the correct dynamics to use is needed. This is especially important in order to be able to do a complete cosmological perturbation theory, for example to explain the cosmic microwave background data.

of one element containing  $N_1$  elements and probability of the past lightcone of another element containing  $N_2$  elements, when the two elements have partially overlapping pasts. At a practical level, as we will see below, knowledge of these correlations is needed in order to make the calculation of the fluctuations we are interested in more tractable. More generally, however, these correlations give us a deeper understanding of the causal set itself. The quantities we work with and whose correlations we discuss depend on causal intervals (of different cardinalities) and such intervals are ubiquitous in causal set theory.

This paper is structured as follows. We begin with a review of causal set theory and Poisson sprinkling in Section 2. In Section 3 we define two useful functions (the cardinality indicator  $\zeta$  and the occupation indicator  $\chi$ ) for accounting for correlations. In the same section we also discuss the three different types of correlations that result from self and cross correlations between these two functions, i.e.,  $\zeta - \zeta$ ,  $\chi - \chi$ , and  $\zeta - \chi$  correlations. Section 4 reviews the definition and properties of the causal set action and its potential connection to Everpresent  $\Lambda$ . Finally, in Section 5 we use our formalism to set up, simplify, and calculate the fluctuations of the causal set action. We conclude in Section 6 with a discussion of the utility of our formalism and future directions of this work. There are also three appendices: Appendix A contains explicit expressions for some of the correlation functions that appear in this paper, and Appendix B contains further details on products of the  $\chi$ -function. Finally, Appendix C contains examples of parametrizations of some of the relevant integrals.

## 2 Causal Sets and Poisson Sprinkling

For causal sets that are well approximated by continuum spacetimes, the Poisson distribution provides a statistical dictionary between causal set quantities and their counterpart continuum quantities. Below we review the basics of causal set theory and the Poisson distribution and show how to use the Poisson distribution to make statistical statements.

### 2.1 Causal Set Theory

The causal set approach to quantum gravity postulates that spacetime is inherently discrete, with the discrete elements and the causal relations between them serving as fundamental building blocks. Causal sets obey a set of basic principles which we now outline. A *causal set* (or *causet*) is a set  $\mathcal{C}$  with a partial order relation  $\preceq$  that is

1. Reflexive: for all  $x \in \mathcal{C}$ ,  $x \preceq x$ .
2. Antisymmetric: for all  $x, y \in \mathcal{C}$ ,  $x \preceq y$  and  $y \preceq x$  implies  $x = y$ .
3. Transitive: for all  $x, y, z \in \mathcal{C}$ ,  $x \preceq y$  and  $y \preceq z$  implies  $x \preceq z$ .
4. Locally finite: for all  $x, z \in \mathcal{C}$ , the cardinality of the set  $\{y \in \mathcal{C} \mid x \preceq y \preceq z\}$  is finite.

We write  $x \prec y$  if  $x \preceq y$  and  $x \neq y$ . The set  $\mathcal{C}$  corresponds to the collection of spacetime elements, while the order relation  $\preceq$  signifies the causal precedence relation between these

elements. Conditions 1-3 are satisfied by points in continuum spacetimes as well, while condition 4 entails the discreteness of causal sets.

Classically, the aim of the causal set approach is that, at large scales, a smooth and continuous manifold will emerge from the underlying discrete causal set, and the Einstein equations would be recovered as an effective description (see e.g. [19, 30, 31] and references therein). In general, however, it is not always possible to embed a given causal set in a manifold and it is an open question how *manifoldlike* causal sets would emerge dynamically.<sup>3</sup> Setting aside this question, it is known how to generate (kinematically rather than dynamically) manifoldlike causal sets that are approximated by any given Lorentzian manifold of interest. The recipe for doing so involves the Poisson distribution, and the process of creating a causal set in this way is referred to as performing a Poisson sprinkling (or sprinkling in short).

In the sprinkling process, one starts with a known spacetime – described by a manifold  $\mathcal{M}$  with Lorentzian metric  $g_{ab}$  – and according to a *Poisson process* randomly places points in the given spacetime such that the number of elements in any arbitrary region with spacetime volume  $V$  follows a Poisson distribution. We elaborate on the properties of the Poisson distribution in the next subsection. This uniform but random distribution of elements according to the sprinkling is in some sense the most strategic placement of a finite number of elements within a continuum spacetime in order to sample arbitrary volumes well. The sprinkled elements are then endowed with the causal relations according to the causal structure of the continuum spacetime into which they were sprinkled, thus satisfying conditions 1-4 above.

## 2.2 Poisson Sprinkling

Having established the importance of the Poisson distribution in generating manifoldlike causal sets, let us take a closer look at the definition of this distribution and its consequences for causal set sprinklings produced by it.

As mentioned above, a sprinkling generates a causal set that is well approximated by a continuum spacetime by placing points at random in that spacetime manifold via a Poisson process<sup>4</sup> such that the probability to find  $i$  elements in a region  $\mathcal{R}$  with spacetime volume

---

<sup>3</sup>Some progress in this direction was made in [32–34].

<sup>4</sup>One can think of the Poisson process as dividing spacetime into small subregions with volume  $dV$  and placing at most one point in each subregion, with probability  $\rho dV$ . The probability to place a point in each subregion is *independent of other subregions*. Then, the probability of there being  $i$  points in a region with volume  $V$  is  $P_i(V) = \binom{V/dV}{i} (\rho dV)^i (1 - \rho dV)^{V/dV - i}$  which becomes (2.1) when  $dV \rightarrow 0$ , according to the Poisson limit theorem [35, 36].  $\binom{V/dV}{i}$  is the number of ways to pick  $i$  subregions from the total number of subregions which is  $V/dV$ ,  $(\rho dV)^i$  is the probability to have an element in those  $i$  subregions, and the last factor is the probability to not have elements in the remaining  $V/dV - i$  subregions. Note that the probability in a submanifold will also converge to the Poisson distribution due to the independence of the point placements in this Poisson process.

$V_{\mathcal{R}}$  is given by the Poisson distribution [37]

$$P_i(V_{\mathcal{R}}) = \frac{(\rho V_{\mathcal{R}})^i}{i!} e^{-\rho V_{\mathcal{R}}}, \quad (2.1)$$

where  $\rho$  is the average (constant) density of points in the region. We will only work with finite spacetime volumes and regions. This distribution is the defining property of a causal set sprinkling. Much of what we discuss subsequently is either a direct or indirect consequence of (2.1) being the probability distribution of the number of causal set elements in  $V_{\mathcal{R}}$ . Let us review some of these consequences below.

For any region  $\mathcal{R} \subseteq \mathcal{M}$ , we can define a number operator

$$\text{Num}_{\mathcal{R}}(\mathcal{C}) \equiv \text{Number of elements of } \mathcal{C} \text{ in the region } \mathcal{R}. \quad (2.2)$$

As a result of and by the definition of the Poisson distribution (2.1), the mean and standard deviation of  $\text{Num}_{\mathcal{R}}$  are

$$\langle \text{Num}_{\mathcal{R}} \rangle = \sum_{i=0}^{\infty} i P_i(V_{\mathcal{R}}) = \rho V_{\mathcal{R}}, \quad (2.3)$$

and

$$\Delta \text{Num}_{\mathcal{R}} = \sqrt{\langle \text{Num}_{\mathcal{R}}^2 \rangle - \langle \text{Num}_{\mathcal{R}} \rangle^2} = \sqrt{\sum_{i=0}^{\infty} i^2 P_i(V_{\mathcal{R}}) - \left( \sum_{i=0}^{\infty} i P_i(V_{\mathcal{R}}) \right)^2} = \sqrt{\rho V_{\mathcal{R}}}, \quad (2.4)$$

respectively. Hence, the statistics of  $\text{Num}_{\mathcal{R}}$  are straightforward to determine through the Poisson distribution which it follows according to (2.1). But what about the statistics of other causal set quantities (in sprinklings) other than  $\text{Num}_{\mathcal{R}}$ ? Such quantities will not necessarily be distributed according to the Poisson distribution, but their statistics will nevertheless be a consequence of  $\text{Num}_{\mathcal{R}}$  following a Poisson distribution. To understand the distributions of more general quantities, it is helpful to reformulate the statistics in terms of an ensemble  $\text{Sp}[\mathcal{M}]$  of causal sets produced by repeated Poisson sprinklings (with the same density) of a spacetime manifold  $\mathcal{M}$ ,

$$\text{Sp}[\mathcal{M}] = \{\mathcal{C}_1, \mathcal{C}_2, \dots\}. \quad (2.5)$$

For simplicity, we assume that the ensemble is very large but finite, such that we capture the properties of the Poisson distribution to a good approximation.<sup>5</sup> Given a function  $f : \text{Sp}[\mathcal{M}] \rightarrow \mathbb{R}$ , its average over the ensemble of Poisson sprinklings is<sup>6</sup>

$$\langle f \rangle \equiv \frac{1}{|\text{Sp}[\mathcal{M}]|} \sum_{\mathcal{C} \in \text{Sp}[\mathcal{M}]} f(\mathcal{C}). \quad (2.6)$$

---

<sup>5</sup>Note that the ensemble of sprinklings is infinitely large if the Poisson distribution, and some of the properties we will discuss, are to hold exactly.

<sup>6</sup>For an infinite ensemble, the definition would be

$$\langle f \rangle \equiv \lim_{n \rightarrow \infty} \frac{1}{n} \sum_{\mathcal{C} \in \text{Sp}^{(n)}[\mathcal{M}]} f(\mathcal{C}),$$

where  $\text{Sp}^{(n)}[\mathcal{M}] \equiv \{\mathcal{C}_1, \dots, \mathcal{C}_n\}$  is a truncation of the sprinklings to the first  $n$  causal sets (according to some ordering).

For example, if  $f(\mathcal{C}) = \text{Num}_{\mathcal{R}}(\mathcal{C})$  in (2.6), we would recover (2.3). More generally, however, since the probability distributions of generic quantities in sprinklings are not known or do not have closed form expressions, (2.6) describes their statistics.

A useful function which we will use throughout this paper is the Kronecker delta function  $\delta_{\text{Num}_{\mathcal{R}}(\mathcal{C}),i}$  which evaluates to 1 if there are  $i$  elements of the causal set  $\mathcal{C}$  in the spacetime region  $\mathcal{R}$  with spacetime volume  $V_{\mathcal{R}}$ , and evaluates to 0 otherwise. Then the probability of having  $i$  elements in the region with volume  $V_{\mathcal{R}}$  is given by the average of  $\delta_{\text{Num}_{\mathcal{R}},i}$  over the ensemble (2.5)

$$\langle \delta_{\text{Num}_{\mathcal{R}},i} \rangle = \frac{1}{|\text{Sp}[\mathcal{M}]|} \sum_{\mathcal{C} \in \text{Sp}[\mathcal{M}]} \delta_{\text{Num}_{\mathcal{R}}(\mathcal{C}),i} = P_i(V_{\mathcal{R}}), \quad (2.7)$$

i.e. the Poisson distribution (2.1). Note that from the definitions above, the following operator identities hold

$$\sum_{i=0}^{\infty} \delta_{\text{Num}_{\mathcal{R}}(\mathcal{C}),i} = 1, \quad (2.8)$$

and

$$\text{Num}_{\mathcal{R}}(\mathcal{C}) = \sum_{i=0}^{\infty} i \delta_{\text{Num}_{\mathcal{R}}(\mathcal{C}),i}. \quad (2.9)$$

The first one implies that  $P_i(V_{\mathcal{R}})$  is normalized, while the second one implies the relation (2.3).

### 3 Correlations Between Quantities in Different Regions

A calculation we will often encounter is to determine the expectation of finding  $N_1$  elements in region  $\mathcal{R}_1$  and  $N_2$  elements in region  $\mathcal{R}_2$ . If  $\mathcal{R}_1$  and  $\mathcal{R}_2$  are overlapping regions, and we will often find that they are, the expectation for there being  $N_1$  elements in region  $\mathcal{R}_1$  *depends* on the likelihood of there being  $N_2$  elements in region  $\mathcal{R}_2$ . As a consequence, to correctly compute the joint expectation, we must take into account the correlation between these two abundances. In the next two subsections we will introduce some notation and machinery that will help us perform computations of such correlation functions. In the third subsection we will apply this machinery to calculate correlations.

#### 3.1 The $\zeta$ -function (Cardinality Indicator)

In the computation of the fluctuations of the causal set action (see Section 5), we will often need an indicator for whether a causal set sprinkling  $\mathcal{C}$  in a particular region  $\mathcal{R}$  has  $i$  elements. In this section we will introduce the *Cardinality Indicator* function,  $\zeta$ , for this purpose. We also explore some of its formal properties, as these will play an important role in our calculations.

The Cardinality Indicator function  $\zeta_i$  ( $i \geq 0$ ) for a causal set  $\mathcal{C}$  and region  $\mathcal{R}$  is defined as<sup>7</sup>

$$\zeta_i^{\mathcal{C}}(\mathcal{R}) \equiv \delta_{\text{Num}_{\mathcal{R}}(\mathcal{C}),i}. \quad (3.1)$$

---

<sup>7</sup>Note that this is merely the delta function we had introduced earlier in (2.7), but given a new name.



It is useful to introduce a special variant when the region is a causal diamond<sup>8</sup>  $\mathcal{R} = I(x, y)$

$$\zeta_i^{\mathcal{C}}(x, y) \equiv \Theta_{x,y} \zeta_i^{\mathcal{C}}(I(x, y)), \quad (3.2)$$

where<sup>9</sup>

$$\Theta_{x,y} \equiv \begin{cases} 1 & \text{if } I(x, y) \neq \emptyset, \\ 0 & \text{otherwise.} \end{cases} \quad (3.3)$$

In other words, (3.2) tells us if there are  $i$  elements in  $I(x, y)$  only if the interval  $I$  actually exists. Note that in our convention,  $x, y \notin I(x, y)$ . If  $x$  and  $y$  are elements in  $\mathcal{C}$  we can also write

$$\zeta_i^{\mathcal{C}}(x, y) = \begin{cases} 1 & \text{if } y \in \diamond_{i+1}(x), \\ 0 & \text{otherwise.} \end{cases}, \quad (3.4)$$

where  $\diamond_i(x)$  is the set of elements  $y$  that causally precede  $x$  ( $y \prec x$ ) and have  $i-1$  elements in the causal diamond between  $x$  and  $y$  (excluding  $x$  and  $y$  themselves). Therefore,  $\diamond_1(x)$  would be a nearest neighbour element. For later convenience we will define  $\diamond_0(x) \equiv \{x\}$ , however note that  $x \notin \diamond_i(x)$  for  $i > 0$ .

With this function we can conveniently define domains such as

$$\sum_{y \in \diamond_{i+1}(x)} f(y) = \sum_{y \in \mathcal{J}^-(x)} f(y) \zeta_i^{\mathcal{C}}(x, y), \quad (3.5)$$

for  $i \geq 0$ . This is useful as it is one of the ingredients needed to express sums over causal sets in terms of integrals over manifolds.

### 3.1.1 General Properties of $\zeta$

If a non-empty region  $\mathcal{R}$  is split into  $n$  disjoint (possibly empty) subregions<sup>10</sup>

$$\mathcal{R} = \bigsqcup_{a=1}^n \mathcal{R}_a, \quad (3.6)$$

then we have the *Disjoint Decomposition Property*

$$\zeta_i^{\mathcal{C}}\left(\bigsqcup_{a=1}^n \mathcal{R}_a\right) = \sum_{\substack{\alpha_a \geq 0 \\ \alpha_1 + \dots + \alpha_n = i}} \prod_{a=1}^n \zeta_{\alpha_a}^{\mathcal{C}}(\mathcal{R}_a), \quad (3.7)$$

where the right hand side sums over all possible ways of distributing  $i$  elements in the  $n$  subregions of  $\mathcal{R}$ . Either one of the terms in the sum is 1 and the rest are 0, or all are 0, i.e.

<sup>8</sup>Here we define a causal diamond as  $I(x, y) = \mathcal{J}^-(x) \cap \mathcal{J}^+(y)$ , where  $\mathcal{J}^+(x) = \{z | x \prec z\}$  and  $\mathcal{J}^-(x) = \{z | z \prec x\}$ . Note that  $x \prec y$  also implies  $x \neq y$  and therefore  $x \notin \mathcal{J}^{\pm}(x)$ . By abuse of notation, we will often use these regions to either mean submanifolds of  $\mathcal{M}$  or subsets of its sprinkling  $\mathcal{C}$ .

<sup>9</sup>Note that in the definition of  $\Theta_{x,y}$ ,  $I(x, y)$  is a submanifold of spacetime, i.e. not a subset of the causal set.

<sup>10</sup>Any shared boundary between subregions would be considered as part of only one of the subregions.

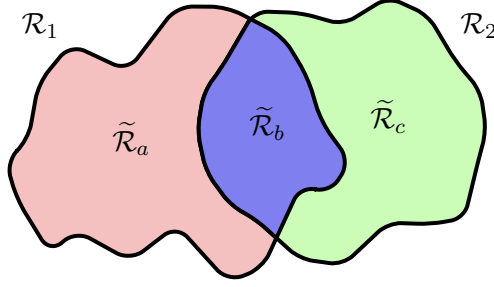


**Figure 1.** Two non-empty regions  $\mathcal{R}_1$  and  $\mathcal{R}_2$  with non-empty overlap  $\tilde{\mathcal{R}}_b = \mathcal{R}_1 \cap \mathcal{R}_2$ . The union  $\mathcal{R}_1 \cup \mathcal{R}_2$  can be decomposed into non-overlapping subregions  $\tilde{\mathcal{R}}_b$ ,  $\tilde{\mathcal{R}}_a = \mathcal{R}_1 \setminus \tilde{\mathcal{R}}_b$  and  $\tilde{\mathcal{R}}_c = \mathcal{R}_2 \setminus \tilde{\mathcal{R}}_b$ .

there is at most one non-zero contribution to the sum (3.7) for a given causal set  $\mathcal{C}$ . For example, for two subregions  $\mathcal{R} = \mathcal{R}_1 \sqcup \mathcal{R}_2$  we have

$$\begin{aligned} \zeta_i^{\mathcal{C}}(\mathcal{R}_1 \sqcup \mathcal{R}_2) &= \sum_{\alpha=0}^i \zeta_{\alpha}^{\mathcal{C}}(\mathcal{R}_1) \zeta_{i-\alpha}^{\mathcal{C}}(\mathcal{R}_2), \\ &= \sum_{\alpha=0}^i \delta_{\text{Num}_{\mathcal{R}_1}(\mathcal{C}), \alpha} \delta_{\text{Num}_{\mathcal{R}_2}(\mathcal{C}), i-\alpha}. \end{aligned} \quad (3.8)$$

Now, we want to address the following problem. Imagine  $n$  regions  $\mathcal{R}_1, \dots, \mathcal{R}_n$ , which are potentially overlapping. We would like to decompose a product of  $\zeta$ -functions of the form

$$\zeta_{i_1}^{\mathcal{C}}(\mathcal{R}_1) \cdots \zeta_{i_n}^{\mathcal{C}}(\mathcal{R}_n), \quad (3.9)$$

into sums of

$$\zeta_{\alpha}^{\mathcal{C}}(\tilde{\mathcal{R}}_a) \zeta_{\beta}^{\mathcal{C}}(\tilde{\mathcal{R}}_b) \zeta_{\gamma}^{\mathcal{C}}(\tilde{\mathcal{R}}_c) \cdots, \quad (3.10)$$

where the potentially overlapping regions have been decomposed into disjoint regions  $\tilde{\mathcal{R}}$

$$\mathcal{R}_1 \cup \cdots \cup \mathcal{R}_n = \tilde{\mathcal{R}}_a \sqcup \tilde{\mathcal{R}}_b \sqcup \tilde{\mathcal{R}}_c \cdots. \quad (3.11)$$

In order to see how this is done, consider two non-empty regions  $\mathcal{R}_1$  and  $\mathcal{R}_2$  with overlap  $\tilde{\mathcal{R}}_b = \mathcal{R}_1 \cap \mathcal{R}_2$ . The union can be decomposed into disjoint regions as (see Figure 1)

$$\mathcal{R}_1 \cup \mathcal{R}_2 = \tilde{\mathcal{R}}_a \sqcup \tilde{\mathcal{R}}_b \sqcup \tilde{\mathcal{R}}_c, \quad (3.12)$$

where  $\tilde{\mathcal{R}}_a = \mathcal{R}_1 \setminus \tilde{\mathcal{R}}_b$  and  $\tilde{\mathcal{R}}_c = \mathcal{R}_2 \setminus \tilde{\mathcal{R}}_b$ . Note that some of these regions can be empty<sup>11</sup>. The first step is to use the Disjoint Decomposition Property (3.7) for  $\mathcal{R}_1 = \tilde{\mathcal{R}}_a \sqcup \tilde{\mathcal{R}}_b$  and  $\mathcal{R}_2 = \tilde{\mathcal{R}}_c \sqcup \tilde{\mathcal{R}}_b$ :

$$\zeta_i^{\mathcal{C}}(\mathcal{R}_1) = \sum_{\alpha=0}^i \delta_{\text{Num}_{\tilde{\mathcal{R}}_a}(\mathcal{C}), \alpha} \delta_{\text{Num}_{\tilde{\mathcal{R}}_b}(\mathcal{C}), i-\alpha}, \quad (3.13)$$

$$\zeta_j^{\mathcal{C}}(\mathcal{R}_2) = \sum_{\gamma=0}^j \delta_{\text{Num}_{\tilde{\mathcal{R}}_c}(\mathcal{C}), \gamma} \delta_{\text{Num}_{\tilde{\mathcal{R}}_b}(\mathcal{C}), j-\gamma}. \quad (3.14)$$

<sup>11</sup>For example when there is no overlap between regions  $\mathcal{R}_1$  and  $\mathcal{R}_2$ .

Multiplying these two expressions gives us the constraint  $i - \alpha = j - \gamma \equiv \beta$ , and we can thus write

$$\begin{aligned} \zeta_i^{\mathcal{C}}(\mathcal{R}_1)\zeta_j^{\mathcal{C}}(\mathcal{R}_2) &= \sum_{\substack{\alpha,\beta,\gamma \geq 0 \\ \alpha+\beta=i \\ \beta+\gamma=j}} \delta_{\text{Num}_{\tilde{\mathcal{R}}_a}(\mathcal{C}),\alpha} \delta_{\text{Num}_{\tilde{\mathcal{R}}_b}(\mathcal{C}),\beta} \delta_{\text{Num}_{\tilde{\mathcal{R}}_c}(\mathcal{C}),\gamma} \\ &= \sum_{\substack{\alpha,\beta,\gamma \geq 0 \\ \alpha+\beta=i \\ \beta+\gamma=j}} \zeta_{\alpha}^{\mathcal{C}}(\tilde{\mathcal{R}}_a) \zeta_{\beta}^{\mathcal{C}}(\tilde{\mathcal{R}}_b) \zeta_{\gamma}^{\mathcal{C}}(\tilde{\mathcal{R}}_c). \end{aligned} \quad (3.15)$$

This is the decomposition we sought. For many overlapping regions, similar decompositions can be derived using the property (3.15).

### 3.2 The $\chi$ -function (Occupation Indicator)

It turns out that besides the  $\zeta$ -function, we also need the *Occupation Indicator* function,  $\chi$ , which indicates whether a region  $\mathcal{R}$  contains (*is occupied by*) elements in the sprinkling  $\mathcal{C}$ . As we will see below (e.g. (3.21)), this function is useful as it allows us to translate between a continuum manifold and a corresponding sprinkling of it.

The  $\chi$ -function is defined as

$$\chi^{\mathcal{C}}(\mathcal{R}) \equiv \sum_{i=1}^{\infty} \zeta_i^{\mathcal{C}}(\mathcal{R}) = \begin{cases} 1 & \text{if } \text{Num}_{\mathcal{R}}(\mathcal{C}) > 0, \\ 0 & \text{otherwise.} \end{cases} \quad (3.16)$$

We are primarily interested in the case where the regions are infinitesimal,  $\delta\mathcal{R}$ , and we would like to find an explicit expression for  $\chi^{\mathcal{C}}(\delta\mathcal{R})$ .

Consider an arbitrary point  $x \in \mathcal{M}$ , not necessarily in  $\mathcal{C}$ , in the interior of a small region  $\Delta\mathcal{R}_x$  with volume  $a^d$ . The  $\lim_{a \rightarrow 0} \chi^{\mathcal{C}}(\Delta\mathcal{R}_x)$  leads to an integration measure  $\chi^{\mathcal{C}}(\delta\mathcal{R}_x)$  which we can find from

$$\begin{aligned} \chi^{\mathcal{C}}(\delta\mathcal{R}_x) &\equiv \lim_{a \rightarrow 0} \chi^{\mathcal{C}}(\Delta\mathcal{R}_x) = \lim_{a \rightarrow 0} \sum_{i=1}^{\infty} \frac{\delta_{\text{Num}_{\Delta\mathcal{R}_x}(\mathcal{C}),i}}{\Delta V_x} \Delta V_x \\ &= \lim_{a \rightarrow 0} \frac{\delta_{\text{Num}_{\Delta\mathcal{R}_x}(\mathcal{C}),1}}{\Delta V_x} \Delta V_x, \end{aligned} \quad (3.17)$$

where in the second line we have used the fact that in the limit  $\Delta\mathcal{R}_x \rightarrow \delta\mathcal{R}_x$ , there can be at most one element in each cell. The factor  $\delta_{\text{Num}_{\Delta\mathcal{R}_x}(\mathcal{C}),1}$  is a delta function that checks whether  $x$  is in the causal set  $\mathcal{C}$ . This can be expressed using Dirac delta functions as

$$\chi^{\mathcal{C}}(\delta\mathcal{R}_x) = \lim_{a \rightarrow 0} \chi^{\mathcal{C}}(\Delta\mathcal{R}_x) = \sum_{z \in \mathcal{C}} \delta^{(d)}(z - x) dV_x. \quad (3.18)$$

By explicit integration, we can readily see that<sup>12</sup>

$$\int_{\mathcal{R}} \chi^{\mathcal{C}}(\delta\mathcal{R}_x) = \text{Num}_{\mathcal{R}}(\mathcal{C}). \quad (3.20)$$

---

<sup>12</sup>Alternatively, this expression can also be derived in a different way. Consider a discretization of a region  $\mathcal{R} \subseteq \mathcal{M}$ , which we will call  $\Lambda_a(\mathcal{R})$ , where  $a$  is the lattice spacing. Each cell around the lattice point  $x \in \Lambda_a(\mathcal{R})$  (Wigner-Seitz cell [38]) is denoted  $\Delta\mathcal{R}_x$ , with volume  $\Delta V_x = a^d$  in a  $d$ -dimensional cubic lattice.

Essentially,  $\chi^{\mathcal{C}}(\delta\mathcal{R}_x)$  acts as a microscope that locally detects whether a point  $x$  is contained in the sprinkling  $\mathcal{C}$ . This integration measure will be useful for expressing sums of a given Poisson sprinkling of a manifold  $\mathcal{R} \subseteq \mathcal{M}$  as an integral

$$\int_{\mathcal{R}} f(x) \chi^{\mathcal{C}}(\delta\mathcal{R}_x) = \sum_{z \in \mathcal{C}} f(z). \quad (3.21)$$

By taking the average of (3.20) over many sprinklings and using (2.3) we get

$$\left\langle \int_{\mathcal{R}} \chi^{\mathcal{C}}(\delta\mathcal{R}_x) \right\rangle = \langle \text{Num}_{\mathcal{R}}(\mathcal{C}) \rangle = \rho V_{\mathcal{R}}, \quad (3.22)$$

where  $V_{\mathcal{R}}$  is the spacetime volume of  $\mathcal{R}$ . In particular, for infinitesimal regions  $\mathcal{R} = \delta\mathcal{R}_x$  we have

$$\langle \chi^{\mathcal{C}}(\delta\mathcal{R}_x) \rangle = \rho dV_x, \quad (3.23)$$

where  $dV_x$  is the spacetime volume of  $\delta\mathcal{R}_x$ . For simplicity, in the rest of the paper we will often use the notation

$$\chi^{\mathcal{C}}(dV_x) \equiv \chi^{\mathcal{C}}(\delta\mathcal{R}_x). \quad (3.24)$$

### 3.3 Correlation Functions

We are generally interested in computing correlation functions of the form<sup>13</sup>

$$\langle \zeta_{i_1}(x_1, y_1) \cdots \zeta_{i_n}(x_n, y_n) \chi(dV_{x_1}) \chi(dV_{y_1}) \cdots \chi(dV_{x_n}) \chi(dV_{y_n}) \rangle. \quad (3.25)$$

If all of these functions are uncorrelated, (3.25) will split into

$$\langle \zeta_{i_1}(x_1, y_1) \rangle \cdots \langle \zeta_{i_n}(x_n, y_n) \rangle \langle \chi(dV_{x_1}) \rangle \langle \chi(dV_{y_1}) \rangle \cdots \langle \chi(dV_{x_n}) \rangle \langle \chi(dV_{y_n}) \rangle, \quad (3.26)$$

which can simply be evaluated using

$$\langle \zeta_i(x_j, y_j) \rangle = P_i(V_j), \quad \text{and} \quad \langle \chi(dV_x) \rangle = \rho dV_x, \quad (3.27)$$

which were given in (2.7) and (3.23). Here  $V_j$  is the volume of the causal interval  $I(x_j, y_j)$  and  $P_i(V)$  is (2.1).

However, as pointed out in [39], a splitting like (3.26) is not always possible as the functions can be correlated. Below we discuss various types of correlations and outline a strategy to compute these correlation functions.

---

It is clear that the following relation must hold

$$\lim_{a \rightarrow 0} \sum_{x \in \Lambda_a(\mathcal{R})} \chi^{\mathcal{C}}(\Delta\mathcal{R}_x) = \text{Num}_{\mathcal{R}}(\mathcal{C}), \quad (3.19)$$

since in the infinitesimal limit  $\Delta\mathcal{R}_x \rightarrow \delta\mathcal{R}_x$ , there can be at most one element in each cell.

<sup>13</sup>From here onwards we omit the superscript  $\mathcal{C}$  for notational simplicity.

**$\zeta$ - $\zeta$  correlations.** Consider the correlation function  $\langle \zeta_{i_1} \cdots \zeta_{i_n} \rangle$ , which gives the probability of having  $i_1$  elements in  $\mathcal{R}_1$ ,  $i_2$  elements in  $\mathcal{R}_2$  and so on. If we work with non-empty causal diamonds  $\mathcal{R}_1 = I(x_1, y_1), \dots, \mathcal{R}_n = I(x_n, y_n)$ , such that none of them overlap, i.e. pairwise  $\mathcal{R}_i \cap \mathcal{R}_j = \emptyset$ , then these probabilities are independent.<sup>14</sup> In other words, the  $\zeta$  functions are uncorrelated and split in the following manner

$$\langle \zeta_{i_1}(x_1, y_1) \cdots \zeta_{i_n}(x_n, y_n) \rangle = \langle \zeta_{i_1}(x_1, y_1) \rangle \cdots \langle \zeta_{i_n}(x_n, y_n) \rangle. \quad (3.28)$$

However, if the regions overlap then there will be correlations. By using the decomposition properties discussed in Section 3.1.1, we can decompose any product of  $\zeta$ -functions into expressions depending only on non-overlapping regions, such as in (3.15). The correlation function can then be computed by applying (3.28), termwise.

**$\chi$ - $\chi$  correlations.** Next consider the correlation function  $\langle \chi(dV_{x_1}) \cdots \chi(dV_{x_n}) \rangle$ . Once again, if all the regions are non-overlapping, then all the  $\chi$ 's are uncorrelated and we have

$$\langle \chi(dV_{x_1}) \cdots \chi(dV_{x_n}) \rangle = \langle \chi(dV_{x_1}) \rangle \cdots \langle \chi(dV_{x_n}) \rangle. \quad (3.29)$$

This is because sprinklings in neighbourhoods of different points are independent. However, if two points coincide, there are correlations. This can be simply evaluated by noting that  $\chi^n = \chi$ , since it only takes the values 0 or 1. In other words

$$\langle \chi(dV_x)^n \rangle = \langle \chi(dV_x) \rangle \neq \langle \chi(dV_x) \rangle^n. \quad (3.30)$$

**$\zeta$ - $\chi$  correlations.** Finally, let us consider correlations between  $\zeta$  and  $\chi$ . Here we have that

$$\langle \zeta_i(x, y) \chi(dV_z) \rangle = \begin{cases} \langle \zeta_i(x, y) \rangle \langle \chi(dV_z) \rangle & \text{if } z \notin I(x, y), \\ \langle \zeta_{i-1}(x, y) \rangle \langle \chi(dV_z) \rangle & \text{if } z \in I(x, y). \end{cases} \quad (3.31)$$

This can be seen as follows. The correlation function above computes the probability that  $i$  elements are sprinkled in the causal interval  $I(x, y)$  and an element at  $z$ . If  $z \notin I(x, y)$ , then the two functions are uncorrelated since the probability of sprinkling in each region is independent. If  $z \in I(x, y)$ , then the functions are correlated. We can still split the joint probability into a product of probabilities, if we turn the  $\zeta$  probability into a conditional probability. For example, in (3.31), in the second line on the right hand side we have expressed this as the probability of there being one element at  $z$  times the probability of there being  $i$  elements in  $I(x, y)$  *given that* there is an element within  $I(x, y)$ . The latter (to lowest order in  $dV_x$ ) is the probability for there being  $i - 1$  elements in  $I(x, y)$ .<sup>15</sup> We give a more careful treatment of this case in Section 3.3.2.

We can also use (3.31) to handle more general correlation functions such as

$$\langle \zeta_i(x, y) \chi(dV_z) \cdots \rangle = \langle \zeta_{i-1}(x, y) \cdots \rangle \langle \chi(dV_z) \rangle, \quad (3.32)$$

---

<sup>14</sup>This follows from the independence of the Poisson process, and the fact that we are taking the average over a (large enough) ensemble of Poisson sprinklings.

<sup>15</sup>This can also be seen by using (2.6), with the definitions of  $\chi$  and  $\zeta$ . The goal is to find which fraction of the terms in the sum contribute to the average.

where  $\dots$  are any other products of  $\zeta$ 's and  $\chi$ 's that are uncorrelated with  $\chi(dV_z)$ .

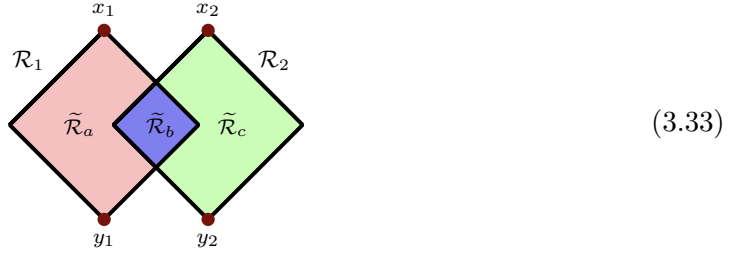
To summarize the overall strategy to compute a correlation function (3.25):

1. First resolve  $\chi - \chi$  correlations using  $\chi^n = \chi$ , for coinciding points.
2. Then resolve  $\zeta - \chi$  correlations, by pulling out one  $\chi$  at a time using (3.31).
3. Finally, resolve  $\zeta - \zeta$  correlations using the decomposition (3.15) and (3.28).

### 3.3.1 Example Calculations

In this section, we compute correlation functions of the form (3.25) using the strategy outlined above.

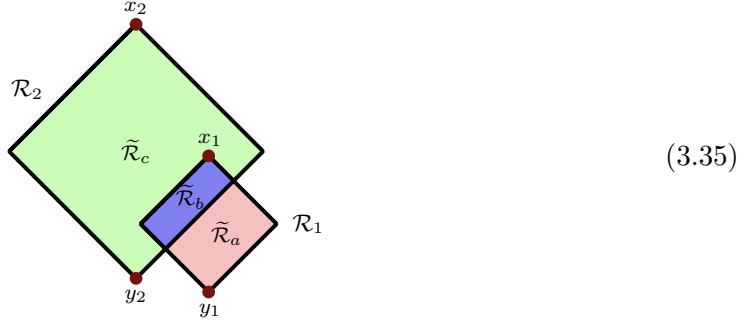
Let us consider the  $\zeta - \zeta$  correlation for the case illustrated below



We first use (3.15) to decompose in terms of non-overlapping regions  $\tilde{\mathcal{R}}_a, \tilde{\mathcal{R}}_b$  and  $\tilde{\mathcal{R}}_c$ , and then we use (3.28) for the non-overlapping regions (step 3 of the strategy). We find

$$\begin{aligned}
\langle \zeta_i(x_1, y_1) \zeta_j(x_2, y_2) \rangle &= \sum_{\substack{\alpha, \beta, \gamma \geq 0 \\ \alpha + \beta = i \\ \beta + \gamma = j}} \langle \zeta_\alpha(\tilde{\mathcal{R}}_a) \zeta_\beta(\tilde{\mathcal{R}}_b) \zeta_\gamma(\tilde{\mathcal{R}}_c) \rangle \\
&= \sum_{\substack{\alpha, \beta, \gamma \geq 0 \\ \alpha + \beta = i \\ \beta + \gamma = j}} \langle \zeta_\alpha(\tilde{\mathcal{R}}_a) \rangle \langle \zeta_\beta(\tilde{\mathcal{R}}_b) \rangle \langle \zeta_\gamma(\tilde{\mathcal{R}}_c) \rangle \\
&= \sum_{\substack{\alpha, \beta, \gamma \geq 0 \\ \alpha + \beta = i \\ \beta + \gamma = j}} P_\alpha(V_a) P_\beta(V_b) P_\gamma(V_c).
\end{aligned}
\tag{3.34}$$

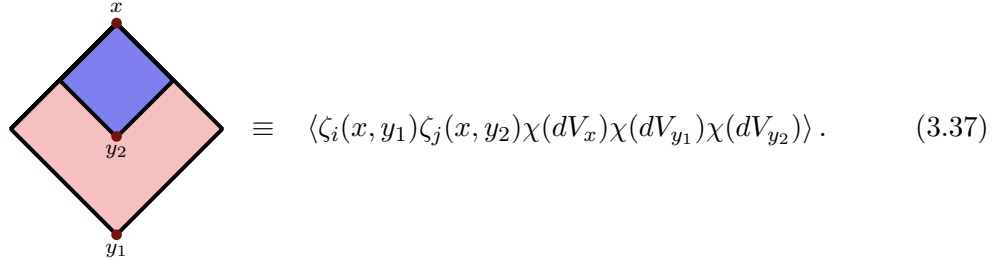
Here  $V_a, V_b$  and  $V_c$  are the volumes of the regions  $\tilde{\mathcal{R}}_a, \tilde{\mathcal{R}}_b$  and  $\tilde{\mathcal{R}}_c$ , respectively. There can be additional subtleties when both  $\chi$  and  $\zeta$  functions are present in the correlation functions, due to possible  $\zeta - \chi$  correlations. For example, let us consider the  $\langle \zeta_i(x_1, y_1) \zeta_j(x_2, y_2) \chi(dV_{x_1}) \rangle$  correlation in the example below



As a result of  $x_1 \in \mathcal{R}_2$ ,  $\chi(dV_{x_1})$  and  $\zeta_j(x_2, y_2)$  are correlated. We use step 2 in the [strategy](#) to resolve the  $\chi - \zeta$  correlation, and then step 3 for the remaining  $\zeta - \zeta$  correlation.

$$\begin{aligned}
\langle \zeta_i(x_1, y_1) \zeta_j(x_2, y_2) \chi(dV_{x_1}) \rangle &= \langle \zeta_i(x_1, y_1) \zeta_{j-1}(x_2, y_2) \rangle \langle \chi(dV_{x_1}) \rangle \\
&= \sum_{\substack{\alpha, \beta, \gamma \geq 0 \\ \alpha + \beta = i \\ \beta + \gamma = j - 1}} \langle \zeta_\alpha(\tilde{\mathcal{R}}_a) \rangle \langle \zeta_\beta(\tilde{\mathcal{R}}_b) \rangle \langle \zeta_\gamma(\tilde{\mathcal{R}}_c) \rangle \langle \chi(dV_{x_1}) \rangle \\
&= \rho \sum_{\substack{\alpha, \beta, \gamma \geq 0 \\ \alpha + \beta = i \\ \beta + \gamma = j - 1}} P_\alpha(V_a) P_\beta(V_b) P_\gamma(V_c) dV_{x_1}.
\end{aligned} \tag{3.36}$$

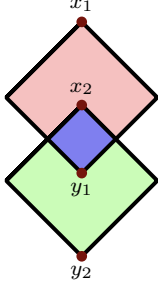
Similarly, we can deal with more complicated correlation functions. We can graphically represent the correlation functions in the following way: a causal diamond between  $x$  and  $y$  represents a  $\zeta_i(x, y)$  and each red dot at  $z$  represents a  $\chi(dV_z)$ . For example



The  $i$  and  $j$  indices are not explicit in this graphical representation. By applying the three steps in our [strategy](#), we can compute these correlations. For example, decomposing analogously to the above examples and using (2.1) we get

$$= \frac{(\rho V_a)^{i-j-1} (\rho V_b)^j}{(i-j-1)! j!} e^{-\rho V_1} \rho^3 dV_x dV_{y_1} dV_{y_2}, \tag{3.38}$$

and

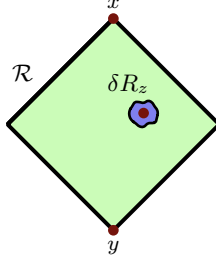


$$= \sum_{\substack{\alpha, \beta, \gamma \geq 0 \\ \alpha + \beta = i - 1 \\ \beta + \gamma = j - 1}} \frac{(\rho V_a)^\alpha (\rho V_b)^\beta (\rho V_c)^\gamma}{\alpha! \beta! \gamma!} e^{-\rho |V_1 \cup V_2|} \rho^4 dV_{x_1} dV_{y_1} dV_{x_2} dV_{y_2}. \quad (3.39)$$

Note that  $V_1$  and  $V_2$  are the volumes of the two diamonds  $\mathcal{R}_1$  and  $\mathcal{R}_2$ , as in (3.33) (see also Figure 1). For convenience, in Appendix A we present explicit expressions for a set of correlation functions that we will need in this work.

### 3.3.2 Careful Treatment of $\zeta - \chi$ Correlations

In order to show the formula (3.31), consider the correlator  $\langle \zeta_i(x, y) \chi(dV_z) \rangle$  where  $z \in I(x, y)$



We can evaluate this using the decomposition (3.15) by noting that

$$\chi(\delta\mathcal{R}_z) = \zeta_1(\delta\mathcal{R}_z) \quad (3.40)$$

for infinitesimal regions, since there can at most be one element there. In other words, only the first term of (3.16) contributes. In this case, the decomposition into disjoint regions (3.12) becomes

$$\mathcal{R} \cup \delta\mathcal{R}_z = \tilde{\mathcal{R}}_a \sqcup \tilde{\mathcal{R}}_b \sqcup \tilde{\mathcal{R}}_c, \quad (3.41)$$

where  $\mathcal{R} = I(x, y)$  and  $\delta\mathcal{R}_z$  is the infinitesimal region around the point  $z$ . Here  $\tilde{\mathcal{R}}_a = \mathcal{R} \setminus \delta\mathcal{R}_z$ ,  $\tilde{\mathcal{R}}_b = \delta\mathcal{R}_z$  and  $\tilde{\mathcal{R}}_c = \emptyset$ . Using (3.40) and applying (3.15) for this decomposition we get

$$\begin{aligned} \langle \zeta_i(x, y) \chi(\delta\mathcal{R}_z) \rangle &= \langle \zeta_i(x, y) \zeta_1(\delta\mathcal{R}_z) \rangle \\ &= \sum_{\substack{\alpha, \beta, \gamma \geq 0 \\ \alpha + \beta = i \\ \beta + \gamma = 1}} \langle \zeta_\alpha(\tilde{\mathcal{R}}_a) \rangle \langle \zeta_\beta(\tilde{\mathcal{R}}_b) \rangle \langle \zeta_\gamma(\tilde{\mathcal{R}}_c) \rangle \\ &= \langle \zeta_{i-1}(\mathcal{R} \setminus \delta\mathcal{R}_z) \rangle P_1(dV_z), \end{aligned} \quad (3.42)$$



where in the second line it was used that since  $\widetilde{\mathcal{R}}_c = \emptyset$ , we must have  $\gamma = 0$ . Expanding the Poisson distribution (2.1) to first order

$$P_1(dV) = \rho dV + O(\rho^2 dV^2). \quad (3.43)$$

Similarly  $\langle \zeta_{i-1}(\mathcal{R} \setminus \delta \mathcal{R}_z) \rangle = P_{i-1}(V - dV_z) = P_{i-1}(V) + O(\rho dV)$ . Therefore, to first order in  $\rho dV$ , (3.42) becomes (3.31).

## 4 Causal Set Action

Thus far we have reviewed the basics of causal set theory and Poisson sprinklings, and discussed how to compute correlation functions in sprinkled regions. For the remainder of the paper, we will focus on the causal set action and we will apply what we have discussed so far, as well as develop additional tools, specifically for the action. In this section we review the definition and properties of the causal set action.

Finding the correct quantum dynamics for causal sets is an important outstanding question. The sum over histories approach to quantum theory, due to its spacetime nature, is a natural formalism for this. While a fundamentally motivated action for causal sets is not yet at hand, e.g. to insert in  $\sum_{\mathcal{C}} e^{iS[\mathcal{C}]}$ , there exist a few candidate proposals for actions that possess some of the desired properties. One thing the action and the dynamics that ensue from it must ultimately explain is how manifoldlike causal sets, approximated by solutions to Einstein's equations, emerge macroscopically. This is highly non-trivial given that non-manifoldlike causal sets vastly outnumber manifoldlike ones [10]. As stated in [19], the *nonlocality* of causal sets will play a key role in making possible the emergence of causal sets approximated by spacetimes described by General Relativity.

The Benincasa-Dowker-Glaser (BDG) action [19, 40] is one of the most interesting and useful constructions of an Einstein-Hilbert-like action in terms of quantities intrinsic to causal sets. It was derived somewhat indirectly, through studies of nonlocal analogs of d'Alembertian operators that describe the propagation of scalar fields on causal sets. Studies of these d'Alembertians in causal sets approximated by curved spacetimes, revealed that they (on average) produce a term approximated by the Ricci scalar curvature in addition to a term approximated by the local d'Alembertian. The BDG action [19, 40] in  $d$  spacetime dimensions on a causal set  $\mathcal{C}$  is

$$S^{(d)}[\mathcal{C}] = \sum_{x \in \mathcal{C}} B^{(d)} \phi(x), \quad (4.1)$$

where the expression above needs to be evaluated at the constant<sup>16</sup>  $\phi(x) = -2\ell^2/\alpha_d$ ,  $\ell$  is the discreteness scale, and  $B^{(d)}$  is the d'Alembertian or Box operator [18, 19, 40–42] defined as

$$B^{(d)} \phi(x) = \frac{1}{\ell^2} \left( \alpha_d \phi(x) + \beta_d \sum_{i=1}^{n_d} c_i \sum_{y \in \diamond_i(x)} \phi(y) \right), \quad (4.2)$$

---

<sup>16</sup>For notational ease, we keep the  $\phi(x)$  unevaluated in some expressions below.

where  $c_i$ ,  $\alpha_d$  and  $\beta_d$  are constants (fixed to ensure that the continuum limit of the average of  $B$  over sprinklings agrees with  $\square$ ), and  $n_d$  is an integer. We remind the reader that  $y \in \diamond_i(x)$  indicates that  $y$  causally precedes  $x$  ( $y \prec x$ ) and that there are  $i - 1$  elements in the causal diamond between  $x$  and  $y$  (excluding  $x$  and  $y$  themselves). Therefore,  $\diamond_1(x)$  would be a nearest neighbour. In the continuum limit ( $\rho \rightarrow \infty$ ), the mean of  $B$  (in any dimension) over all Poisson sprinklings into a spacetime can be approximated by the usual local d'Alembertian,  $\square$ , plus a term proportional to the Ricci scalar curvature [19, 43]:

$$\lim_{\rho \rightarrow \infty} \langle B \phi(x) \rangle = \left( \square - \frac{1}{2} R(x) \right) \phi(x). \quad (4.3)$$

The  $1/2$  coefficient of  $R$  is universal [41] (i.e. independent of spacetime dimension). The right hand side of (4.3) is the reason why the BDG action is defined via (4.1). Recently, a set of higher order curvature invariants were also constructed in a similar manner [44]. An explicit example of a nonlocal d'Alembertian operator in  $3 + 1$ D is [45–47]

$$B^{(4)} \phi(x) = \frac{4}{\sqrt{6} \ell^2} \left( -\phi(x) + \left( \sum_{i=1}^3 c_i \sum_{y \in \diamond_i} \right) \phi(y) \right), \quad (4.4)$$

with coefficients  $c_1 = 1, c_2 = -9, c_3 = 16, c_4 = -8$ . The values of the coefficients  $\{c_i\}$  vary from one definition of nonlocal d'Alembertian to another (see e.g. [46]). However, a common feature among the different sets of  $c_i$ 's is that their values alternate in sign for odd and even indices  $i$ . Thus we can regard the d'Alembertian and action constructed in this way to in some sense obey an inclusion-exclusion principle. It is precisely this inclusion-exclusion principle, via the alternating signs, that creates the necessary cancellations to approximate local quantities using nonlocal inputs.

As mentioned, the mean of  $B$  when averaged over an ensemble of Poisson sprinkled causal sets, is approximated by the usual local d'Alembertian  $\square$  plus a term proportional to  $R(x)$ . By the same token, the BDG action (4.1), when averaged over many causal sets, is approximated by the Einstein-Hilbert action. However, there are fluctuations away from the mean of the action for individual causal set realizations of the same continuum spacetime. These are the fluctuations that we will study below. Partly to tame these fluctuations, a more general one-parameter family of nonlocal BDG actions has also been defined, where a nonlocality scale  $\ell_k > \ell$  (recall that  $\ell$  is the discreteness scale) damps out the fluctuations below this scale for any single causal set [19, 45]. This results in an action that is approximated by the Einstein-Hilbert action for any particular sprinkled causal set without the need for averaging.

The cosmological constant  $\Lambda$  and the gravitational action are closely related. The cosmological constant enters the classical gravitational action as

$$S_G = \int \left[ \frac{1}{16\pi G} (R - 2\Lambda) \right] \sqrt{-g} d^d x + \text{Boundary terms}, \quad (4.5)$$

and in the causal set case, the analog of this would be

$$S_C = \sum_{x \in \mathcal{C}} R(x) - 2\Lambda V + \text{Boundary terms}, \quad (4.6)$$

where by  $R(x)$  in (4.6) we mean the action of  $B$  on (an appropriately normalized) constant, and by  $V$  we mean  $N/\rho$ , i.e. the expressions in terms of causal set quantities. The cosmological constant term in (4.6) is not present in the average of the BDG action over causal sets, but perhaps the fluctuations in  $S$  defined on a single causal set could be identified with this term. As mentioned in the introduction, there is a model of a stochastic cosmological constant, known as Everpresent  $\Lambda$  [20, 22, 23, 48], that is motivated by principles of causal set theory. According to the model, the value of the cosmological constant fluctuates over cosmic history, with a standard deviation at each epoch that is of the order of  $1/\sqrt{V}$  where  $V$  is the spacetime volume at that epoch. The magnitude of these fluctuations is related to the Poisson distribution that describes the relation between number and volume in manifoldlike causal sets. This Everpresent  $\Lambda$  idea did not stem from an action definition. However as we can see from (4.6), it is very natural for it to be related to an action. Moreover, since we observe fluctuations in the BDG action (4.1), and since the cosmological constant in Everpresent  $\Lambda$  also fluctuates, it begs the question of whether there may be a potential connection between the two fluctuations. Investigating this connection may also give us deeper insight into the properties of Everpresent  $\Lambda$ , and furnish some missing pieces in current phenomenological models of it (such as what the value of the mean is about which fluctuations occur). This is one of the main motivations for focusing our investigations on fluctuations of the action, in this paper. The fluctuations of  $\Lambda$  in Everpresent  $\Lambda$  have a quantum origin but we aim to connect these fluctuations to statistical ones due to the Poisson distribution, in the same spirit as other heuristics on this subject (see e.g. the discussion in Section 3 of [23]).

We devote the next section to discussing the mean and fluctuations of the BDG family of nonlocal actions, over an ensemble of Poisson sprinkled causal sets.

## 5 Fluctuations of the Causal Set Action

The aim of this section is to compute the fluctuations of the action, given by the variance

$$(\Delta S)^2 = \langle S^2 \rangle - \langle S \rangle^2, \quad (5.1)$$

where the  $\langle \cdot \rangle$  are the averages with respect to an ensemble of Poisson sprinklings (2.6) of a spacetime manifold  $\mathcal{M}$ . The expectation value  $\langle S \rangle$  was computed in [49] and [50]. We will here briefly review how to compute  $\langle S \rangle$  using our formalism and then outline how to compute  $\langle S^2 \rangle$ .

For simplicity of notation we first rewrite the Box operator (4.2) as

$$B^{(d)}\phi(x) = \frac{1}{\ell^2} \sum_{i=0}^{n_d} C_i^{(d)} \sum_{y \in \diamond_i(x)} \phi(y), \quad (5.2)$$

where

$$C_i^{(d)} = \begin{cases} \alpha_d, & i = 0 \\ \beta_d c_i^{(d)}, & i \neq 0 \end{cases}. \quad (5.3)$$

The expectation value of the action (4.1) is then given by

$$\langle S \rangle = -\frac{2}{\alpha_d} \sum_{i=0}^{n_d} C_i^{(d)} \left\langle \sum_{x \in \mathcal{C}} \sum_{y \in \diamond_i(x)} \right\rangle = -\frac{2}{\alpha_d} \sum_{i=0}^{n_d} C_i^{(d)} \mathcal{L}_{i-1}, \quad (5.4)$$

where we have made the substitution  $\phi(x) = -2\ell^2/\alpha_d$  above, and where

$$\mathcal{L}_i \equiv \left\langle \sum_{x \in \mathcal{C}} \sum_{y \in \diamond_{i+1}(x)} \right\rangle. \quad (5.5)$$

Note that the index  $i$  in  $\mathcal{L}_i$  spans the range  $i = -1, \dots, n_d - 1$ , as this will turn out to be more convenient later. Similarly, for  $S^2$  we can express the expectation value as

$$\begin{aligned} \langle S^2 \rangle &= \frac{4}{\alpha_d^2} \sum_{i,j=0}^{n_d} C_i^{(d)} C_j^{(d)} \left\langle \sum_{x_1, x_2 \in \mathcal{C}} \sum_{y_1 \in \diamond_i(x_1)} \sum_{y_2 \in \diamond_j(x_2)} \right\rangle, \\ &= \frac{4}{\alpha_d^2} \sum_{i,j=0}^{n_d} C_i^{(d)} C_j^{(d)} \mathcal{K}_{i-1j-1}, \end{aligned} \quad (5.6)$$

where we have defined the correlation matrix

$$\mathcal{K}_{ij} \equiv \left\langle \sum_{x_1, x_2 \in \mathcal{C}} \sum_{y_1 \in \diamond_{i+1}(x_1)} \sum_{y_2 \in \diamond_{j+1}(x_2)} \right\rangle. \quad (5.7)$$

This matrix is clearly symmetric

$$\mathcal{K}_{ij} = \mathcal{K}_{ji}, \quad (5.8)$$

and we do not need to compute all of its elements. We will from now on only consider the elements  $i \leq j$ . Also note that the domains of the sums inside the expectation value are mutually correlated and depend on  $\mathcal{C}$ , and therefore cannot be taken out of the expectation value.

In conclusion, the fluctuations are given by

$$(\Delta S)^2 = \frac{4}{\alpha_d^2} \sum_{i,j=0}^{n_d} C_i^{(d)} C_j^{(d)} \mathcal{M}_{i-1j-1}, \quad (5.9)$$

where

$$\mathcal{M}_{ij} = \mathcal{K}_{ij} - \mathcal{L}_i \mathcal{L}_j. \quad (5.10)$$

## 5.1 Integral Formulation

In order to evaluate the expectation values  $\mathcal{L}_i$  and  $\mathcal{K}_{ij}$ , it is convenient to reformulate them as integrals over various submanifolds of  $\mathcal{M}$ . The tools needed to achieve this were developed in Section 3.

We start by using (3.5) for  $i > 0$ ,

$$\sum_{y \in \diamond_i(x)} = \begin{cases} 1 & i = 0, \\ \sum_{y \in \mathcal{J}^-(x)} \zeta_{i-1}^{\mathcal{C}}(x, y) & i > 0, \end{cases} \quad (5.11)$$

to remove the  $i$  (and causal set) dependence in the domain of the sum. Now we can readily use (3.21) to express the sums over causal set elements  $x$  and  $y$  (the left hand side below) as integrals over generic points  $x$  and  $y$  in the continuum spacetime (the right hand side below)

$$\sum_{x \in \mathcal{C}} \sum_{y \in \diamond_i(x)} = \begin{cases} \int_{\mathcal{M}} \chi^{\mathcal{C}}(dV_x) & i = 0, \\ \int_{\mathcal{M}} \int_{\mathcal{J}^-(x)} \zeta_{i-1}^{\mathcal{C}}(x, y) \chi^{\mathcal{C}}(dV_y) \chi^{\mathcal{C}}(dV_x) & i > 0. \end{cases} \quad (5.12)$$

Note that the domains of the integrals only depend on the manifold  $\mathcal{M}$ , while the dependence on the particular sprinkling  $\mathcal{C}$  is hidden in the measures  $\chi^{\mathcal{C}}(dV_x)$  and  $\chi^{\mathcal{C}}(dV_y)$ . This measure can concretely be written as (3.18).

Using (5.12) in (5.5) and (5.7), we then find the following integral expressions for the expectations values

$$\mathcal{L}_i = \begin{cases} \int_{\mathcal{M}} \langle \chi^{\mathcal{C}}(dV_x) \rangle & i = -1, \\ \int_{\mathcal{M}} \int_{\mathcal{J}^-(x)} \langle \zeta_i^{\mathcal{C}}(x, y) \chi^{\mathcal{C}}(dV_y) \chi^{\mathcal{C}}(dV_x) \rangle & i \geq 0, \end{cases} \quad (5.13)$$

and

$$\mathcal{K}_{ij} = \begin{cases} \int_{\mathcal{M}} \int_{\mathcal{M}} \langle \chi^{\mathcal{C}}(dV_{x_1}) \chi^{\mathcal{C}}(dV_{x_2}) \rangle, & i = j = -1 \\ \int_{\mathcal{M}} \int_{\mathcal{M}} \int_{\mathcal{J}^-(x_2)} \langle \zeta_j^{\mathcal{C}}(x_2, y_2) \chi^{\mathcal{C}}(dV_{y_2}) \chi^{\mathcal{C}}(dV_{x_1}) \chi^{\mathcal{C}}(dV_{x_2}) \rangle, & i = -1, j \geq 0 \\ \int_{\mathcal{M}} \int_{\mathcal{M}} \int_{\mathcal{J}^-(x_2)} \int_{\mathcal{J}^-(x_1)} \langle \zeta_i^{\mathcal{C}}(x_1, y_1) \zeta_j^{\mathcal{C}}(x_2, y_2) \chi^{\mathcal{C}}(dV_{y_1}) \chi^{\mathcal{C}}(dV_{y_2}) \chi^{\mathcal{C}}(dV_{x_1}) \chi^{\mathcal{C}}(dV_{x_2}) \rangle, & i, j \geq 0 \end{cases} \quad (5.14)$$

Note that the integration domains are independent of any particular sprinkling and can thus be pulled out of the averaging. The integrands need to be evaluated before the integrals can be performed. This problem can be readily solved using the formalism and techniques developed earlier in this paper, specifically the [strategy](#) in Section 3.3. In particular by using (3.31), (3.29) and (3.27) we find

$$\mathcal{L}_i = \begin{cases} \rho V_{\mathcal{M}} & i = -1, \\ \frac{\rho^2}{i!} \int_{\mathcal{M}} \int_{\mathcal{J}^-(x)} (\rho V_{xy})^i e^{-\rho V_{xy}} dV_y dV_x & i \geq 0, \end{cases} \quad (5.15)$$

where  $V_{xy}$  is the spacetime volume of the causal diamond  $I(x, y)$ . For  $i \geq 0$  we actually only need to compute a single integral

$$\mathcal{L} \equiv \int_{\mathcal{M}} \int_{\mathcal{J}^-(x)} e^{-\rho V_{xy}} dV_y dV_x, \quad (5.16)$$

since

$$\begin{aligned}\mathcal{L}_i &= \frac{\rho^{i+2}}{i!} \left[ -\frac{d}{d\rho} \right]^i \left[ \int_{\mathcal{M}} \int_{\mathcal{J}^-(x)} e^{-\rho V_{xy}} dV_y dV_x \right] \\ &= \frac{\rho^{i+2}}{i!} \left[ -\frac{d}{d\rho} \right]^i \mathcal{L}.\end{aligned}\tag{5.17}$$

This observation will turn out to be more general, and dramatically reduce the number of independent integrals needed to be evaluated.

For  $\mathcal{K}_{ij}$  the computation of the integrands is more subtle, as different regions of the integration domain have different kinds of correlations. It is therefore necessary to split the integration domain into submanifolds, based on the type of correlation involved, and compute each separately. The rest of this section, is dedicated to this task.

## 5.2 Special Case $\mathcal{K}_{-1,j}$

In (5.14) we split the (symmetric) correlation matrix into three cases. Before dealing with general components of this matrix, it is instructive to separately consider the first two cases,  $\mathcal{K}_{-1,-1}$  and  $\mathcal{K}_{-1,j}$ , to understand the nature of these calculations.

### 5.2.1 $\mathcal{K}_{-1,-1}$

We want to compute

$$\mathcal{K}_{-1,-1} = \int_{\mathcal{M}} \int_{\mathcal{M}} \langle \chi(dV_{x_1}) \chi(dV_{x_2}) \rangle.\tag{5.18}$$

As noted in Section 3.3, there are  $\chi - \chi$  correlations only when  $x_1 = x_2$ . We can thus split the integral into a region where  $x_1 = x_2$  and another where  $x_1 \neq x_2$ , with the integrands reducing to  $\langle \chi(dV_x) \rangle$  and  $\langle \chi(dV_x) \rangle \langle \chi(dV_{x_2}) \rangle$ , respectively. Using (3.27), this matrix component thus becomes

$$\mathcal{K}_{-1,-1} = \rho V_{\mathcal{M}} + \rho^2 V_{\mathcal{M}}^2.\tag{5.19}$$

The contribution to the fluctuations (5.9) is then

$$\mathcal{M}_{-1,-1} = \rho V_{\mathcal{M}}.\tag{5.20}$$

### 5.2.2 $\mathcal{K}_{-1,j}$

We want to compute

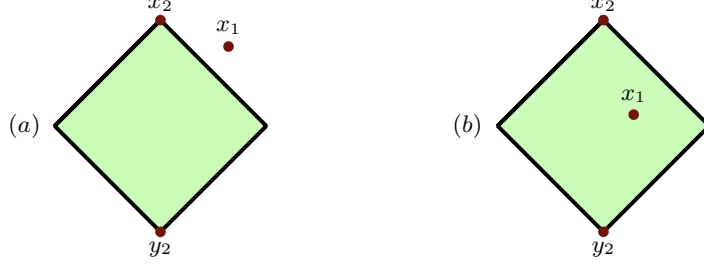
$$\mathcal{K}_{-1,j} = \int_{\mathcal{M}} \int_{\mathcal{M}} \int_{\mathcal{J}^-(x_2)} \langle \zeta_j(x_2, y_2) \chi(dV_{y_2}) \chi(dV_{x_2}) \chi(dV_{x_1}) \rangle\tag{5.21}$$

for  $j \geq 0$ . Now,  $\chi - \chi$  correlations will occur when  $x_1 = x_2$  or when  $x_1 = y_2$ . In both of these cases the integral becomes

$$\int_{\mathcal{M}} \int_{\mathcal{J}^-(x)} \langle \zeta_j(x, y) \rangle \langle \chi(dV_y) \rangle \langle \chi(dV_x) \rangle,\tag{5.22}$$

which is nothing but  $\mathcal{L}_j$  (5.15).

When  $x_1 \neq x_2 \neq y_2$ , we have two scenarios



(a) when  $x_1 \notin I(x_2, y_2)$  and (b) when  $x_1 \in I(x_2, y_2)$ . For (a) we have no  $\zeta - \chi$  correlations and the integral becomes

$$\int_{\mathcal{M}} \int_{\mathcal{J}^-(x_2)} \int_{\mathcal{M} \setminus I(x_2, y_2)} \langle \zeta_j(x_2, y_2) \rangle \langle \chi(dV_{x_1}) \rangle \langle \chi(dV_{y_2}) \rangle \langle \chi(dV_{x_2}) \rangle, \quad (5.23)$$

while for (b) there are  $\zeta - \chi$  correlations and we find

$$\int_{\mathcal{M}} \int_{\mathcal{J}^-(x_2)} \int_{I(x_2, y_2)} \langle \zeta_{j-1}(x_2, y_2) \rangle \langle \chi(dV_{x_1}) \rangle \langle \chi(dV_{y_2}) \rangle \langle \chi(dV_{x_2}) \rangle, \quad (5.24)$$

using the [rules](#) in Section 3.3. Note that, (5.24) only contributes when  $j \geq 1$ . So for  $j = 0$  we get

$$\mathcal{K}_{-1,0} = 2\mathcal{L}_j + \rho^3 \int_{\mathcal{M}} \int_{\mathcal{J}^-(x_2)} \int_{\mathcal{M} \setminus I(x_2, y_2)} e^{-\rho V_{x_2 y_2}} dV_{x_1} dV_{y_2} dV_{x_2}, \quad (5.25)$$

while for  $j > 0$  we have

$$\begin{aligned} \mathcal{K}_{-1,j} = 2\mathcal{L}_j &+ \frac{\rho^{3+j}}{j!} \int_{\mathcal{M}} \int_{\mathcal{J}^-(x_2)} \int_{\mathcal{M} \setminus I(x_2, y_2)} V_{x_2 y_2}^j e^{-\rho V_{x_2 y_2}} dV_{x_1} dV_{y_2} dV_{x_2} \\ &+ \frac{\rho^{3+j-1}}{(j-1)!} \int_{\mathcal{M}} \int_{\mathcal{J}^-(x_2)} \int_{I(x_2, y_2)} V_{x_2 y_2}^{j-1} e^{-\rho V_{x_2 y_2}} dV_{x_1} dV_{y_2} dV_{x_2}. \end{aligned} \quad (5.26)$$

The contribution of these correlations to fluctuations of the action (5.9) becomes

$$\mathcal{M}_{-1,j} = \mathcal{K}_{-1,j} - \rho V_{\mathcal{M}} \mathcal{L}_j. \quad (5.27)$$

### 5.3 General Case $\mathcal{K}_{ij}$

Now we will turn to the general case (5.14) of computing

$$\mathcal{K}_{ij} = \int_{\mathcal{M}} \int_{\mathcal{M}} \int_{\mathcal{J}^-(x_2)} \int_{\mathcal{J}^-(x_1)} \left\langle \zeta_i(x_1, y_1) \zeta_j(x_2, y_2) \chi(dV_{y_1}) \chi(dV_{y_2}) \chi(dV_{x_1}) \chi(dV_{x_2}) \right\rangle, \quad (5.28)$$

for  $i, j \geq 0$ . Just as in the special cases above, we will first deal with the  $\chi - \chi$  correlations, which will split the integral (5.28) into six integrals. In each of these integrals, we will then deal with the  $\zeta - \chi$  and  $\zeta - \zeta$  correlations using the [strategy](#) outlined in Section 3.3.

### 5.3.1 $\chi$ - $\chi$ Correlations

As discussed in Section 3.3, there will be  $\chi - \chi$  correlations in the submanifolds where the  $x_i$ 's and  $y_i$ 's coincide. Before accounting for them, it is instructive to revisit why and how these correlations occur.

Let  $\mathcal{C}$  be a causal set that contains the sprinkled element  $y_1$ . Since  $dV_{y_1}$  is a small region surrounding  $y_1$ , we have by definition (3.16) that  $\chi(dV_{y_1}) = 1$ . For any point  $y_2 \neq y_1$ , there is an infinitesimal probability that there is a sprinkled element in an infinitesimal region around  $y_2$  in  $\mathcal{C}$ . Thus, there is an infinitesimal probability that  $\chi(dV_{y_2}) = 1$ .<sup>17</sup> However, if  $y_1 = y_2$ , then the probability for  $\chi(dV_{y_2}) = 1$  is 1 and there is therefore a correlation between  $\chi(dV_{y_1})$  and  $\chi(dV_{y_2})$ .

It is thus convenient to decompose the integral into six parts

$$\mathcal{K}_{ij} = J_{ij}^1 + J_{ij}^2 + J_{ij}^3 + J_{ij}^4 + J_{ij}^5 + J_{ij}^6, \quad (5.29)$$

depending on which  $\chi - \chi$  correlations are present. See Appendix B for more details on these correlations. Each component in (5.29) is integrated over a subregion defined respectively by

$$J^1 : x_1 = x_2, \quad y_1 = y_2, \quad (5.30a)$$

$$J^2 : x_1 \neq x_2, \quad y_1 = y_2, \quad (5.30b)$$

$$J^3 : x_1 = x_2, \quad y_1 \neq y_2, \quad (5.30c)$$

$$J^4 : x_1 = y_2, \quad x_2 \neq y_1 \quad (5.30d)$$

$$J^5 : x_2 = y_1, \quad x_1 \neq y_2 \quad (5.30e)$$

$$J^6 : x_1 \neq x_2 \neq y_1 \neq y_2. \quad (5.30f)$$

Using (3.30), each component in (5.29) is then given by

$$J_{ij}^1 = \int_{\mathcal{M}} \int_{\mathcal{J}^-(x)} \left\langle \zeta_i(x, y) \zeta_j(x, y) \chi(dV_y) \chi(dV_x) \right\rangle, \quad (5.31)$$

$$J_{ij}^2 = \int_{\mathcal{M}} \int_{\mathcal{M} \setminus \{x_2\}} \int_{\mathcal{J}^-(x_1) \cap \mathcal{J}^-(x_2)} \left\langle \zeta_i(x_1, y) \zeta_j(x_2, y) \chi(dV_y) \chi(dV_{x_1}) \chi(dV_{x_2}) \right\rangle, \quad (5.32)$$

$$J_{ij}^3 = \int_{\mathcal{M}} \int_{\mathcal{J}^-(x)} \int_{\mathcal{J}^-(x) \setminus \{y_2\}} \left\langle \zeta_i(x, y_1) \zeta_j(x, y_2) \chi(dV_{y_1}) \chi(dV_{y_2}) \chi(dV_x) \right\rangle, \quad (5.33)$$

$$J_{ij}^4 = \int_{\mathcal{M}} \int_{\mathcal{J}^-(x)} \int_{\mathcal{J}^-(y_2)} \left\langle \zeta_i(y_2, y_1) \zeta_j(x, y_2) \chi(dV_{y_1}) \chi(dV_{y_2}) \chi(dV_x) \right\rangle, \quad (5.34)$$

$$J_{ij}^5 = \int_{\mathcal{M}} \int_{\mathcal{J}^-(x)} \int_{\mathcal{J}^-(y_1)} \left\langle \zeta_i(x, y_1) \zeta_j(y_1, y_2) \chi(dV_{y_2}) \chi(dV_{y_1}) \chi(dV_x) \right\rangle, \quad (5.35)$$

and

$$J_{ij}^6 = \int_{\mathcal{M}} \int_{\mathcal{M} \setminus \{x_2\}} \int_{\mathcal{J}^-(x_2)} \int_{\mathcal{J}^-(x_1) \setminus \{y_2\}} \left\langle \zeta_i(x_1, y_1) \zeta_j(x_2, y_2) \chi(dV_{y_1}) \chi(dV_{y_2}) \chi(dV_{x_1}) \chi(dV_{x_2}) \right\rangle. \quad (5.36)$$

<sup>17</sup>In other words, the average of  $\chi(dV_{y_2})$  over sprinklings  $\mathcal{C}$  that contain  $y_1$ , is infinitesimal.



Note that

$$J_{ij}^4 = J_{ji}^5, \quad (5.37)$$

as we can see by relabeling the dummy variables in the integrals. Similarly, there may be other  $J_{ij}^a$  components that are equal and therefore the minimal set of independent integrals may be smaller.

### 5.3.2 $\zeta$ - $\chi$ Correlations

Now we will deal with  $\zeta$ - $\chi$  correlations, according to the [discussion](#) in Section 3.3. This will further split the integration domains (5.30) into subregions, with different  $\zeta$ - $\chi$  correlations and thus different integrands. For this, it is convenient to first define the following notation for the integration domains needed

$$\mathcal{D}_1 = \{(x, y) \in \mathcal{M} \times \mathcal{M} \mid y \prec x\}, \quad (5.38a)$$

$$\mathcal{D}_2 = \{(x_1, x_2, y) \in \mathcal{M} \times \mathcal{M} \times \mathcal{M} \mid (y \prec x_1) \wedge (y \prec x_2) \wedge (x_1 \neq x_2)\}, \quad (5.38b)$$

$$\mathcal{D}_3 = \{(x, y_1, y_2) \in \mathcal{M} \times \mathcal{M} \times \mathcal{M} \mid (y_1 \prec x) \wedge (y_2 \prec x) \wedge (y_1 \neq y_2)\}, \quad (5.38c)$$

$$\mathcal{D}_4 = \{(x, y_1, y_2) \in \mathcal{M} \times \mathcal{M} \times \mathcal{M} \mid (y_2 \prec x) \wedge (y_1 \prec y_2)\}, \quad (5.38d)$$

$$\mathcal{D}_5 = \{(x, y_1, y_2) \in \mathcal{M} \times \mathcal{M} \times \mathcal{M} \mid (y_1 \prec x) \wedge (y_2 \prec y_1)\}, \quad (5.38e)$$

$$\mathcal{D}_6 = \{(x_1, x_2, y_1, y_2) \in \mathcal{M}^4 \mid (y_1 \prec x_1) \wedge (y_2 \prec x_2) \wedge (x_1 \neq x_2 \neq y_1 \neq y_2)\} \quad (5.38f)$$

In this notation,  $\mathcal{D}_i$  corresponds to the integration domain of the  $J^i$  integral. We diagrammatically express the additional splittings of the domains  $\mathcal{D}$  due to the  $\zeta$ - $\chi$  correlations as

$$\mathcal{D}_1 = \color{blue}{\diamond}, \quad \mathcal{D}_4 = \color{green}{\diamond} \sqcup \color{red}{\diamond}, \quad \mathcal{D}_5 = \color{red}{\diamond} \sqcup \color{green}{\diamond}, \quad (5.39)$$

where the colors are used as in Section 3.3.1, for example see (3.33). Similarly we have the decomposition

$$\mathcal{D}_2 = \color{green}{\diamond} \sqcup \color{red}{\diamond} \sqcup \color{blue}{\diamond}, \quad (5.40)$$

where each submanifold is

$$\begin{aligned} \color{red}{\diamond} &= \{(x_1, x_2, y) \in \mathcal{D}_2 \mid (x_1 \not\prec x_2) \wedge (x_2 \not\prec x_1)\}, \\ \color{red}{\diamond} &= \{(x_1, x_2, y) \in \mathcal{D}_2 \mid x_2 \prec x_1\}, \\ \color{green}{\diamond} &= \{(x_1, x_2, y) \in \mathcal{D}_2 \mid x_1 \prec x_2\}, \end{aligned} \quad (5.41)$$

and

$$\mathcal{D}_3 = \color{blue}{\diamond} \sqcup \color{red}{\diamond} \sqcup \color{green}{\diamond}, \quad (5.42)$$

where

$$\begin{aligned} \color{blue}{\diamond} &= \{(x, y_1, y_2) \in \mathcal{D}_3 \mid (y_1 \not\prec y_2) \wedge (y_2 \not\prec y_1)\}, \\ \color{red}{\diamond} &= \{(x, y_1, y_2) \in \mathcal{D}_3 \mid y_1 \prec y_2\}, \\ \color{green}{\diamond} &= \{(x, y_1, y_2) \in \mathcal{D}_3 \mid y_2 \prec y_1\}. \end{aligned} \quad (5.43)$$



since

$$J_{ij}^4 = \frac{\rho^{i+j+3}}{i!j!} \left[ -\frac{\partial}{\partial \rho_1} \right]^i \left[ -\frac{\partial}{\partial \rho_2} \right]^j J^4(\rho_1, \rho_2) \Big|_{\rho_1=\rho_2=\rho}. \quad (5.50)$$

As we will see later, this is a special case of a much more general property that will reduce the number of integrals that need to be computed to a small core set. For notational convenience, we can adopt a graphical notation for this integral as

$$J_{ij}^4 = \int \diamond \equiv \int \langle \zeta_i(y_2, y_1) \zeta_j(x, y_2) \chi(dV_{y_1}) \chi(dV_{y_2}) \chi(dV_x) \rangle, \quad (5.51)$$

where the integration domain is defined by the figure and the integrand is defined as a correlation function as discussed in Section 3.3.1, in particular (A.2). In other words, the graphical notation  $\diamond$  denotes both the domain of integration and the correlation function in the integrand. The  $i$  and  $j$  indices are not explicit in this notation and must be read from the left hand side,  $J_{ij}^4$ .

### 5.3.5 The $J^2$ Integral

Let us next consider the  $J^2$  integral

$$J_{ij}^2 = \int_{\mathcal{M}} \int_{\mathcal{M} \setminus \{x_2\}} \int_{\mathcal{J}^-(x_1) \cap \mathcal{J}^-(x_2)} \left\langle \zeta_i(x_1, y) \zeta_j(x_2, y) \chi(dV_y) \chi(dV_{x_1}) \chi(dV_{x_2}) \right\rangle. \quad (5.52)$$

In contrast to the previous two cases considered above,  $\zeta - \chi$  correlations will occur in this case. We showed in (5.40) how to split the relevant domain  $\mathcal{D}_2$  into three parts depending on the presence of such correlations.

$$J_{ij}^2 = \int \left( \diamond \sqcup \diamond \sqcup \diamond \right) \left\langle \zeta_i(x_1, y) \zeta_j(x_2, y) \chi(dV_y) \chi(dV_{x_1}) \chi(dV_{x_2}) \right\rangle. \quad (5.53)$$

Due to  $\zeta - \zeta$  correlations, this can be simplified further. For the diagonal elements  $i = j$ , the integrand vanishes in the region  $\diamond \sqcup \diamond$  because

$$\begin{aligned} \langle \zeta_i(x_1, y) \zeta_i(x_2, y) \chi(dV_{x_1}) \rangle &= 0, & \text{for } (x_1, x_2, y) \in \diamond, \\ \langle \zeta_i(x_1, y) \zeta_i(x_2, y) \chi(dV_{x_2}) \rangle &= 0, & \text{for } (x_1, x_2, y) \in \diamond, \end{aligned} \quad (5.54)$$

as in these cases there will always be at least one more element in one diamond compared to the other. For the off-diagonal elements  $i < j$  we have that

$$\langle \zeta_i(x_1, y) \zeta_j(x_2, y) \chi(dV_{x_2}) \rangle = 0, \quad \text{for } (x_1, x_2, y) \in \diamond, \quad (5.55)$$

since in  $\diamond$  we have  $x_2 \prec x_1$  and therefore  $i > j$  which contradicts our assumption  $i < j$ .<sup>18</sup> In summary, the  $J^2$  integral reduces to

$$J_{ij}^2 = (1 - \delta_{ij}) \int \diamond + \int \diamond, \quad (5.56)$$

where again the graphics denote both the integration domain and correlation function in the integrand.

---

<sup>18</sup>We remind the reader that we are presently only working on the upper triangle of the matrix  $J_{ij}$ , i.e. where  $i < j$ .

### 5.3.6 The $J^6$ Integral

Finally, we turn to the  $J^6$  integral which has the most number of correlations and thus contributions,

$$J_{ij}^6 = \int_{\mathcal{M}} \int_{\mathcal{M} \setminus \{x_2\}} \int_{\mathcal{J}^-(x_2)} \int_{\mathcal{J}^-(x_1) \setminus \{y_2\}} \left\langle \zeta_i(x_1, y_1) \zeta_j(x_2, y_2) \chi(dV_{y_1}) \chi(dV_{y_2}) \chi(dV_{x_1}) \chi(dV_{x_2}) \right\rangle. \quad (5.57)$$

Recall that the relevant domain is

$$\mathcal{D}_6 = \begin{array}{cccccccccccc} \color{red}\diamond & \color{green}\diamond & \sqcup & \color{red}\diamond & \color{green}\diamond & \sqcup & \color{green}\diamond & \color{red}\diamond & \sqcup & \color{green}\diamond & \color{red}\diamond & \sqcup & \color{red}\diamond & \color{green}\diamond & \sqcup & \color{red}\diamond & \color{green}\diamond & \color{blue}\diamond & \color{red}\diamond & \color{green}\diamond & \color{blue}\diamond & \color{green}\diamond & \color{blue}\diamond & \color{green}\diamond \end{array}, \quad (5.58)$$

due to  $\chi - \chi$  correlations. The integral can thus be computed by summing over the integral of each disjoint region, where the integrands are again evaluated as described in Section 3.3 and Appendix A. Depending on the indices  $i$  and  $j$  only a subset of the above terms will contribute. For example due to the same logic as in (5.54),  $\color{blue}\diamond$  never contributes as we are only considering components with  $i \leq j$  whereas  $\int_{\color{red}\diamond}$  is only non-zero for  $i \geq j + 2$ . Similarly, the region  $\color{green}\diamond$  will only contribute when  $i + 2 \leq j$ . In summary, for the diagonal elements  $i \geq 0$  we have

$$J_{ii}^6 = \begin{cases} \int_{\color{red}\diamond} + \int_{\color{green}\diamond}, & i = 0, \\ \int_{\color{red}\diamond} + \int_{\color{red}\diamond \color{green}\diamond} + \int_{\color{green}\diamond \color{red}\diamond} + \int_{\color{green}\diamond \color{blue}\diamond} + \int_{\color{red}\diamond \color{blue}\diamond} + \int_{\color{red}\diamond \color{green}\diamond} + \int_{\color{green}\diamond \color{green}\diamond} + \int_{\color{red}\diamond \color{red}\diamond}, & i \geq 1, \end{cases} \quad (5.59)$$

while for the off-diagonal elements ( $i, j \geq 0$ ) we have

$$J_{ij}^6 = \begin{cases} \int_{\color{red}\diamond} + \int_{\color{red}\diamond \color{green}\diamond} + \int_{\color{green}\diamond \color{red}\diamond} + \int_{\color{green}\diamond \color{blue}\diamond}, & i = 0, j = 1, \\ \int_{\color{red}\diamond} + \int_{\color{red}\diamond \color{green}\diamond} + \int_{\color{green}\diamond \color{red}\diamond} + \int_{\color{green}\diamond \color{blue}\diamond} + \int_{\color{red}\diamond \color{blue}\diamond} + \int_{\color{red}\diamond \color{green}\diamond} + \int_{\color{green}\diamond \color{green}\diamond} + \int_{\color{red}\diamond \color{red}\diamond}, & j = i + 1, i > 0, \\ \int_{\color{red}\diamond} + \int_{\color{red}\diamond \color{green}\diamond} + \int_{\color{green}\diamond \color{red}\diamond} + \int_{\color{green}\diamond \color{blue}\diamond} + \int_{\color{red}\diamond \color{blue}\diamond} + \int_{\color{red}\diamond \color{green}\diamond} + \int_{\color{green}\diamond \color{green}\diamond} + \int_{\color{red}\diamond \color{red}\diamond} + \int_{\color{green}\diamond \color{blue}\diamond}, & j \geq i + 2. \end{cases} \quad (5.60)$$

## 5.4 Core Set of Integrals

In summary, in order to calculate the fluctuations of the action, we see from (5.9) that we need the matrix  $\mathcal{M}_{ij}$ . This was decomposed into  $\mathcal{K}_{ij} - \mathcal{L}_i \mathcal{L}_j$ , and  $\mathcal{K}_{ij}$  into  $J_{ij}^1, \dots, J_{ij}^6$ , and then again these were individually decomposed into integrals over various subregions with associated correlation functions. It thus may appear that many different integrals are needed to compute these fluctuations. However, as we saw in (5.17) and (5.50), computing a single integral is enough to get all the other  $i, j$  elements. It turns out that this can be

done for any region, and the main reason is due to the following property of the Poisson distribution

$$P_i(V) = \frac{\rho^i}{i!} \left[ -\frac{d}{d\rho} \right]^i P_0(V) = \frac{\rho^i}{i!} \left[ -\frac{d}{d\rho} \right]^i e^{-\rho V}. \quad (5.61)$$

As an example, let us consider the region  $\diamond\blacklozenge$ . Define the following integral

$$\begin{aligned} \text{int} [\diamond\blacklozenge] &\equiv \int_{\diamond\blacklozenge} P_0(V_a)_{\rho_a} P_0(V_b)_{\rho_b} P_0(V_c)_{\rho_c} dV_{y_1} dV_{y_2} dV_{x_1} dV_{x_2} \\ &= \int_{\diamond\blacklozenge} e^{-\rho_a V_a - \rho_b V_b - \rho_c V_c} dV_{y_1} dV_{y_2} dV_{x_1} dV_{x_2}, \end{aligned} \quad (5.62)$$

where  $P_0(V_a)_{\rho_a} \equiv e^{-\rho_a V_a}$ . Here  $V_a$ ,  $V_b$  and  $V_c$  are the volumes of the three non-overlapping subregions, as used previously (e.g. see Section 3.3.1). By using the property (5.61) we find

$$\begin{aligned} \text{int}_{\alpha\beta\gamma} [\diamond\blacklozenge] &\equiv \frac{\rho^{\alpha+\beta+\gamma}}{\alpha!\beta!\gamma!} \left[ -\frac{\partial}{\partial\rho_a} \right]^\alpha \left[ -\frac{\partial}{\partial\rho_b} \right]^\beta \left[ -\frac{\partial}{\partial\rho_c} \right]^\gamma \Big|_{\rho_a=\rho_b=\rho_c=\rho} \text{int} [\diamond\blacklozenge], \\ &= \int_{\diamond\blacklozenge} P_\alpha(V_a) P_\beta(V_b) P_\gamma(V_c) dV_{y_1} dV_{y_2} dV_{x_1} dV_{x_2}. \end{aligned} \quad (5.63)$$

As defined earlier, we can use the notation  $\int_{\diamond\blacklozenge}$  to mean an integral over the region  $\diamond\blacklozenge$  with the integrand (A.3). In other words, we can express it as

$$\begin{aligned} \int_{\diamond\blacklozenge} &= \rho^4 \sum_{\alpha\beta\gamma} \int_{\diamond\blacklozenge} P_\alpha(V_a) P_\beta(V_b) P_\gamma(V_c) dV_{y_1} dV_{y_2} dV_{x_1} dV_{x_2}, \\ &= \rho^4 \sum_{\alpha\beta\gamma} \text{int}_{\alpha\beta\gamma} [\diamond\blacklozenge], \end{aligned} \quad (5.64)$$

where the domain of the  $\alpha\beta\gamma$  sum depends on the specific region; for example  $\alpha, \beta, \gamma > 0$ ,  $\alpha + \beta = i$  and  $\beta + \gamma = j$  for this region. Therefore, we can compute  $\int_{\diamond\blacklozenge}$  for any  $i$  and  $j$  from a single integral (5.62).

As another example, for  $\blacklozenge\blacklozenge$  we only need

$$\text{int} [\blacklozenge\blacklozenge] = \int_{\blacklozenge\blacklozenge} e^{-\rho_a V_a - \rho_b V_b - \rho_c V_c} dV_{y_1} dV_{y_2} dV_x, \quad (5.65)$$

since from derivatives of this we can find

$$\begin{aligned} \int_{\blacklozenge\blacklozenge} &= \rho^3 \sum_{\alpha\beta\gamma} \int_{\blacklozenge\blacklozenge} P_\alpha(V_a) P_\beta(V_b) P_\gamma(V_c) dV_{y_1} dV_{y_2} dV_x, \\ &= \rho^3 \sum_{\alpha\beta\gamma} \text{int}_{\alpha\beta\gamma} [\blacklozenge\blacklozenge]. \end{aligned} \quad (5.66)$$

The total number of integrals we need to compute for the action fluctuations, is therefore one for each region appearing in our expressions. Everything we need to compute matrices

such as  $J_{ij}^6$  in (5.60) for all  $i$  and  $j$ , is a core set of relevant single integrals such as (5.62), based on the diagrams appearing in their decompositions.

In Appendix C we show explicit examples of parametrizations of some of these integrals.

## 6 Conclusions and Outlook

We have presented a strategy for calculating fluctuations and correlations in causal set theory. These fluctuations are those of causal set quantities with respect to averaging over an ensemble of Poisson sprinklings of a given spacetime manifold. An example of such a fluctuation would be the standard deviation of the number of elements sprinkled into a region of a manifold with spacetime volume  $V$ ; we know the answer in this case is  $\Delta N = \sqrt{\rho V}$ , but for more general quantities this standard deviation must be computed. The notation and formalism we have laid out in this paper streamline a wide range of calculations of this kind.

We paid particular attention to the correlations involved in and the fluctuations of the causal set action. This action, which is a discrete analogue of the Einstein-Hilbert action, depends on causal intervals between causal set elements and on the number of elements within these intervals or diamonds. Therefore the correlations we needed to take into account, for example to compute the standard deviation of the action, included those between pairs of (potentially overlapping) diamonds with different numbers of elements in them. It also turned out to be crucial to carefully treat the expectation of an element lying in an infinitesimal region – essentially at a point (for example at the endpoints of a causal diamond, in order to form a causal set causal interval). These can induce additional correlations, for example when two diamonds share one or more endpoints.

After careful account of all correlations, we expressed the fluctuations of the action in terms of a core set of integrals that need to be computed. We developed a convenient graphical notation for expressing both the domains of these integrals as well as the correlations they represented. Finally, we showed that for each subregion with a distinct correlation type, there is only one core integral that needs to be computed to obtain the answer for more general index combinations. The fact that we do not need to compute separate integrals for each pair of index values considerably reduces the computational work needed to calculate the fluctuations.

In future work, we will apply the formalism we have developed in this paper to particular spacetime manifolds, to explicitly evaluate the fluctuations. As a starting application we will consider Minkowski spacetime, where the parametrization of the necessary domains would be relatively simpler than in curved spacetimes. We further aim to apply our formalism in Friedman-Robertson-Walker type cosmological spacetimes to address the main question that motivated this work, which is whether or not the fluctuations of the action can be used to model Everpresent  $\Lambda$ . Finally, as we have mentioned already, our work opens the door to a large number of similar calculations of fluctuations of generic causal set quantities. Knowledge of these fluctuations will further inform us about the statistical

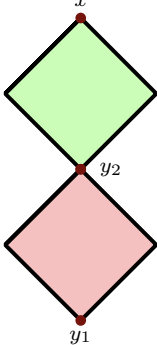
properties of causal sets and can be used in many different contexts such as in questions of dynamics, numerical convergence, and phenomenological model building.

## A Expressions for Correlation Functions

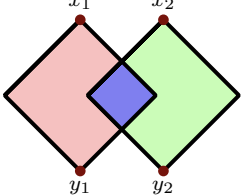
In Section 3.3.1 we developed a simple graphical notation for correlation functions of the type

$$\langle \zeta_i(x_1, y_1) \zeta_j(x_2, y_2) \chi(dV_{x_1}) \chi(dV_{y_1}) \chi(dV_{x_2}) \chi(dV_{y_2}) \rangle, \quad (\text{A.1})$$

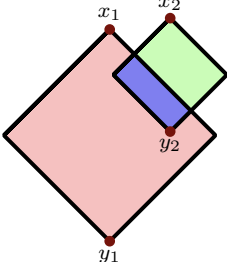
for example see (3.37). For convenience, in this appendix we will provide the explicit evaluations of some of these correlation functions using the basic steps from Section (3.3):



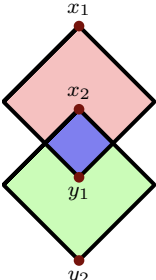
$$= \frac{(\rho V_1)^i (\rho V_2)^j}{i! j!} e^{-\rho |V_1 \cup V_2|} \rho^3 dV_{y_1} dV_{y_2} dV_x, \quad (\text{A.2})$$



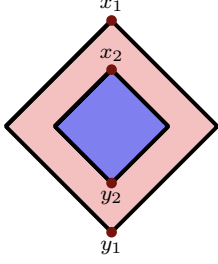
$$= \sum_{\substack{\alpha, \beta, \gamma \geq 0 \\ \alpha + \beta = i \\ \beta + \gamma = j}} \frac{(\rho V_a)^\alpha (\rho V_b)^\beta (\rho V_c)^\gamma}{\alpha! \beta! \gamma!} e^{-\rho |V_1 \cup V_2|} \rho^4 dV_{x_1} dV_{y_1} dV_{x_2} dV_{y_2}, \quad (\text{A.3})$$



$$= \sum_{\substack{\alpha, \beta, \gamma \geq 0 \\ \alpha + \beta + 1 = i \\ \beta + \gamma = j}} \frac{(\rho V_a)^\alpha (\rho V_b)^\beta (\rho V_c)^\gamma}{\alpha! \beta! \gamma!} e^{-\rho |V_1 \cup V_2|} \rho^4 dV_{x_1} dV_{y_1} dV_{x_2} dV_{y_2}, \quad (\text{A.4})$$

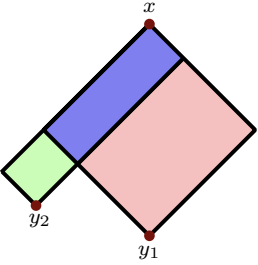


$$= \sum_{\substack{\alpha, \beta, \gamma \geq 0 \\ \alpha + \beta + 1 = i \\ \beta + \gamma + 1 = j}} \frac{(\rho V_a)^\alpha (\rho V_b)^\beta (\rho V_c)^\gamma}{\alpha! \beta! \gamma!} e^{-\rho |V_1 \cup V_2|} \rho^4 dV_{x_1} dV_{y_1} dV_{x_2} dV_{y_2}, \quad (\text{A.5})$$

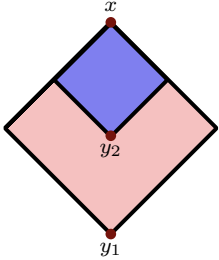


$$= \frac{(\rho V_a)^{i-j-2} (\rho V_b)^j}{(i-j-2)! j!} e^{-\rho V_1} \rho^4 dV_{x_1} dV_{y_1} dV_{x_2} dV_{y_2}. \quad (\text{A.6})$$

Note that (A.6) should be equal to zero when  $i < j + 2$  as this configuration is not possible in the domain above. We take  $\frac{1}{n!}$  to mean  $\frac{1}{\Gamma(n+1)}$ , which yields  $\Gamma(n+1) = \infty$  when  $n$  is a negative integer, making the expression automatically vanish. Further correlations are given by:

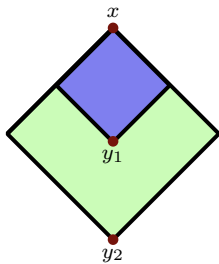


$$= \sum_{\substack{\alpha, \beta, \gamma \geq 0 \\ \alpha + \beta = i \\ \beta + \gamma = j}} \frac{(\rho V_a)^\alpha (\rho V_b)^\beta (\rho V_c)^\gamma}{\alpha! \beta! \gamma!} e^{-\rho |V_1 \cup V_2|} \rho^3 dV_x dV_{y_1} dV_{y_2}, \quad (\text{A.7})$$



$$= \frac{(\rho V_a)^{i-j-1} (\rho V_b)^j}{(i-j-1)! j!} e^{-\rho V_1} \rho^3 dV_x dV_{y_1} dV_{y_2}, \quad (\text{A.8})$$

and



$$= \frac{(\rho V_b)^i (\rho V_c)^{j-i-1}}{(j-i-1)! i!} e^{-\rho V_2} \rho^3 dV_x dV_{y_1} dV_{y_2}. \quad (\text{A.9})$$

## B Products of $\chi$ Functions

The decomposition of (5.28) into (5.29) can be seen more formally in the following way. Using the definition of  $\chi$  in (3.18), we can split the product of the measures into a part



where  $x_1 = x_2$  and a part where  $x_1 \neq x_2$ , i.e.

$$\begin{aligned}
\chi(dV_{x_1})\chi(dV_{x_2}) &= \sum_{z_1 \in \mathcal{C}} \sum_{z_2 \in \mathcal{C}} \delta^{(d)}(z_1 - x_1) \delta^{(d)}(z_2 - x_2) dV_{x_1} dV_{x_2} \\
&= \left[ \sum_{z \in \mathcal{C}} \delta^{(d)}(z - x_1) \delta^{(d)}(z - x_2) + \sum_{z_1 \neq z_2 \in \mathcal{C}} \delta^{(d)}(z_1 - x_1) \delta^{(d)}(z_2 - x_2) \right] dV_{x_1} dV_{x_2}, \\
&= \delta^{(d)}(x_1 - x_2) \chi(dV_{x_1}) dV_{x_2} + \chi(dV_{x_1}, dV_{x_2}),
\end{aligned} \tag{B.1}$$

and similarly for the  $y$  measures

$$\begin{aligned}
\chi(dV_{y_1})\chi(dV_{y_2}) &= \sum_{z_1 \in \mathcal{C}} \sum_{z_2 \in \mathcal{C}} \delta^{(d)}(z_1 - y_1) \delta^{(d)}(z_2 - y_2) dV_{y_1} dV_{y_2} \\
&= \left[ \sum_{z \in \mathcal{C}} \delta^{(d)}(z - y_1) \delta^{(d)}(z - y_2) + \sum_{z_1 \neq z_2 \in \mathcal{C}} \delta^{(d)}(z_1 - y_1) \delta^{(d)}(z_2 - y_2) \right] dV_{y_1} dV_{y_2} \\
&= \delta^{(d)}(y_1 - y_2) \chi(dV_{y_1}) dV_{y_2} + \chi(dV_{y_1}, dV_{y_2}).
\end{aligned} \tag{B.2}$$

Here we have defined the measure

$$\begin{aligned}
\chi(dV_{x_1}, dV_{x_2}) &\equiv \sum_{z_1 \neq z_2 \in \mathcal{C}} \delta^{(d)}(z_1 - x_1) \delta^{(d)}(z_2 - x_2) dV_{x_1} dV_{x_2} \\
&= \left( 1 - \delta^{(d)}(x_1 - x_2) \right) \chi(dV_{x_1}) \chi(dV_{x_2}).
\end{aligned} \tag{B.3}$$

We can more generally define

$$\chi(dV_{x_1}, \dots, dV_{x_n}) \equiv \sum_{z_1 \neq \dots \neq z_n \in \mathcal{C}} \delta^{(d)}(z_1 - x_1) \dots \delta^{(d)}(z_n - x_n) dV_{x_1} \dots dV_{x_n}. \tag{B.4}$$

Essentially,  $\chi(dV_{x_1}, \dots, dV_{x_n})$  represents the product of  $\chi$ 's while enforcing the points to be distinct. Using these, we can further decompose  $\chi(dV_{x_1}, dV_{x_2})\chi(dV_{y_1}, dV_{y_2})$  into subregions where  $\{x_1 = y_2\}$ ,  $\{x_2 = y_1\}$ ,  $\{x_1 = y_1\}$ ,  $\{x_2 = y_2\}$  and  $\{x_1 \neq x_2 \neq y_1 \neq y_2\}$ . In total  $\chi(dV_{x_1})\chi(dV_{x_2})\chi(dV_{y_1})\chi(dV_{y_2})$  splits into 8 terms. By plugging these into (5.28), we recover the six terms in (5.29) while two of the terms ( $\{x_1 = y_1\}$  and  $\{x_2 = y_2\}$ ) vanish due to the integration domain.<sup>19</sup> Finally, we use

$$\chi(dV_{x_1}, \dots, dV_{x_n}) = \chi(dV_{x_1}) \dots \chi(dV_{x_n}), \quad \text{when } x_1 \neq \dots \neq x_n, \tag{B.5}$$

to find the integral forms of  $J^1, \dots, J^6$ .

---


<sup>19</sup>Note that in these cases, the  $\zeta(x, y)$  would also force the integrals to vanish, as the causal diamond between  $x$  and  $y$  would be the empty set (see (3.2)).

## C Parametrization of Integration Domains

In this paper, we reduced the computation of the fluctuations of quantities such as the action to evaluating integrals such as


$$\int_{\text{diamond}}, \quad \int_{\text{diamond}}, \quad \int_{\text{diamond}}, \quad \dots \quad (\text{C.1})$$

This notation might seem abstract, hence in this appendix we illustrate how to evaluate these integrals concretely.

Recall that these diagrams represent all possible submanifolds of  $\mathcal{M} \times \mathcal{M} \times \mathcal{M} \times \mathcal{M}$  where the points  $x_1, y_1, x_2, y_2$  are related as in the diagrams. For example the diagram  which was defined in (5.41) can also be written as

$$\text{diamond} = \{(x_1, x_2, y) \in \mathcal{M}^3 \mid x_1 \in \mathcal{M}, x_2 \in \mathcal{M} \setminus \mathcal{J}^+(x_1) \cup \mathcal{J}^-(x_1) \text{ and } y \in \mathcal{J}^-(x_1) \cap \mathcal{J}^-(x_2)\}. \quad (\text{C.2})$$

In other words, if  $x_1$  is chosen to be any point, then  $x_2$  can be any point that is causally unrelated to  $x_1$  (neither in the past nor future of  $x_1$ ) and  $y$  can be any point in the past of both of them. In the above,  $\mathcal{M} \setminus \mathcal{J}^+(x_1) \cup \mathcal{J}^-(x_1)$  means the manifold  $\mathcal{M}$  with the submanifold  $\mathcal{J}^+(x_1) \cup \mathcal{J}^-(x_1)$  carved out.

Performing the integral over  requires parametrizing all these submanifolds, for a given  $\mathcal{M}$ . However, it turns out that for any diagram one can reduce the needed parametrizations to three types: (1)  $\mathcal{M}$ , (2)  $\mathcal{J}^-(x)$  and (3)  $\mathcal{J}^-(x_1) \cap \mathcal{J}^-(x_2)$ . For example

$$\int_{\text{diamond}} = \int_{\mathcal{M}} \int_{\mathcal{M} \setminus \mathcal{J}^+(x_1) \cup \mathcal{J}^-(x_1)} \int_{\mathcal{J}^-(x_1) \cap \mathcal{J}^-(x_2)} dV_{x_1} dV_{x_2} dV_y, \quad (\text{C.3})$$

can be rewritten as

$$\begin{aligned} \int_{\text{diamond}} &= \int_{\mathcal{M}} \int_{\mathcal{M}} \int_{\mathcal{J}^-(x_1) \cap \mathcal{J}^-(x_2)} dV_{x_1} dV_{x_2} dV_y \\ &\quad - \int_{\mathcal{M}} \int_{\mathcal{J}^-(x_1)} \int_{\mathcal{J}^-(x_2)} dV_{x_1} dV_{x_2} dV_y - \int_{\mathcal{M}} \int_{\mathcal{J}^-(x_2)} \int_{\mathcal{J}^-(x_1)} dV_{x_2} dV_{x_1} dV_y. \end{aligned} \quad (\text{C.4})$$

Here we first take  $x_1$  and  $x_2$  to be unconstrained, then subtract all the contributions from when they are causally related. Note that the last two integrals are equal if the integrand is symmetric in  $x_1$  and  $x_2$ . Other diagrams can also be written in this form.

For concreteness, below we will consider examples of explicit parametrizations of  $\mathcal{J}^-(x)$  and  $\mathcal{J}^-(x_1) \cap \mathcal{J}^-(x_2)$ . In general  $\mathcal{J}^-(x_1) \cap \mathcal{J}^-(x_2)$  is harder to parametrize than  $\mathcal{J}^-(x)$ . For simplicity, we will consider a 1 + 1 dimensional example for  $\mathcal{J}^-(x_1) \cap \mathcal{J}^-(x_2)$ , and a 3 + 1 dimensional example for  $\mathcal{J}^-(x)$ .

### C.1 Example: Parametrization of $\mathcal{J}^-(x_1) \cap \mathcal{J}^-(x_2)$ in a 1 + 1D Minkowski Diamond

Consider the case of a causal diamond  $\mathcal{M} = I(q, p)$  in 1 + 1 dimensional Minkowski space-time. For simplicity, we restrict to pairs of points that are at the same Cartesian time

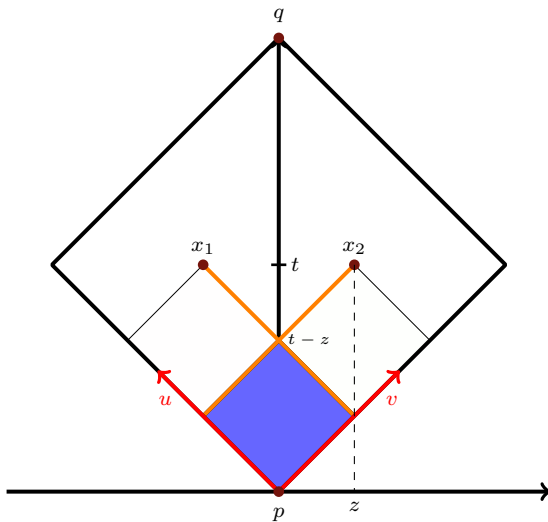


**Figure 2.** Setup of  $\mathcal{J}^-(x_1) \cap \mathcal{J}^-(x_2)$  in a 1 + 1D Minkowski Diamond.

and equal spatial distance (but with opposite sign) from the origin, namely  $x_1 = (t, z)$  and  $x_2 = (t, -z)$ . Let us also place  $p$  at the origin and  $q$  at height  $h$ ,  $q = (h, 0)$ . See Figure 2 for the setup. It is convenient to work in lightcone coordinates  $u$  and  $v$  where

$$u = \frac{1}{\sqrt{2}}(t - z), \quad v = \frac{1}{\sqrt{2}}(t + z). \quad (\text{C.5})$$

In this coordinate system our integral becomes

$$\int_{\mathcal{J}^-(x_1) \cap \mathcal{J}^-(x_2)} f(y) d^2 y = \int_0^{\frac{t-z}{\sqrt{2}}} du \int_0^{\frac{t+z}{\sqrt{2}}} dv f(u, v) \quad (\text{C.6})$$

### C.2 Example: Parametrization of $\mathcal{J}^-(x)$ in a 3 + 1D Minkowski Diamond

Consider a causal diamond  $\mathcal{M} = I(q, p)$  with local Cartesian coordinates (chart)  $Y = (Y^0, \mathbf{Y})$  and metric

$$ds^2 = \eta_{\mu\nu} dY^\mu dY^\nu, \quad (\text{C.7})$$

where  $\eta = \text{diag}(1, -1, -1, -1)$ . In this coordinate system,  $h$  is the height between the top and bottom corners,  $q$  and  $p$ . Their coordinates are  $P = (0, \mathbf{0})_Y$  and  $Q = (h, \mathbf{0})_Y$ .

Let  $x$  be a point in  $\mathcal{M}$  with coordinates  $X = (X^0, \mathbf{X})_Y$ . For any  $x \in \mathcal{M}$ , we are interested in the submanifold  $\mathcal{J}^-(x) = I(x, p) \subset \mathcal{M}$ . In this subsection we will parametrize this submanifold as a function of the points  $p, q$  and  $x$ .<sup>20</sup>

The proper time  $\tau_{px}$  between the points  $p$  and  $x$ , is given by

$$\tau_{px}^2 = (X^0)^2 - \|\mathbf{X}\|^2. \quad (\text{C.8})$$

<sup>20</sup>The treatment in this subsection is similar to the one in [49].

We want to map the point  $y \in I(x, p)$  from  $Y$  coordinates into  $\tilde{Y}$  coordinates such that the interval  $I(x, p)$  in this coordinate system takes the form of a standard upright diamond i.e.  $\tilde{X} = (\tilde{X}^0, \mathbf{0})_{\tilde{Y}}$ ,  $\tilde{P} = (\tilde{P}^0, \mathbf{0})_{\tilde{Y}}$  and

$$\tau_{px}^2 = \left( \tilde{X}^0 - \tilde{P}^0 \right)^2. \quad (\text{C.9})$$

The mapping from  $Y$  to  $\tilde{Y}$  will only use transformations in the Poincaré group  $\mathbb{P} = \mathbb{R}^4 \rtimes SO(3, 1)$  and the metric will therefore remain of the Minkowski form

$$ds^2 = \eta_{\mu\nu} d\tilde{Y}^\mu d\tilde{Y}^\nu. \quad (\text{C.10})$$

In these coordinates, null geodesics will remain straight lines at 45 degrees.

First we bring the origin to  $x$ , using a translation

$$Y^\mu \longrightarrow Y^\mu - X^\mu, \quad (\text{C.11})$$

mapping the points  $p$  and  $x$  to

$$P \longrightarrow P - X = (-X^0, -\mathbf{X}) \quad \text{and} \quad X \longrightarrow X - X = (0, \mathbf{0}). \quad (\text{C.12})$$

We will now use  $SO(3, 1)$  Lorentz-group transformations to bring  $p$  to the form  $\tilde{P} = (\tilde{P}^0, \mathbf{0})_{\tilde{Y}}$ . Such transformations will keep  $\tilde{X} = (0, \mathbf{0})_{\tilde{Y}}$  and thus give us the coordinate system we are seeking.

First we need a rotation  $R \in SO(3) \subset SO(3, 1)$  such that  $p$  has only one non-zero spatial component (say, the  $x$ -direction)

$$P \longrightarrow R(P - X) \stackrel{!}{=} (-X^0, \|\mathbf{X}\|, 0, 0). \quad (\text{C.13})$$

This rotation matrix is given by

$$R = \exp(\theta \mathbf{n} \cdot \mathbf{L}), \quad (\text{C.14})$$

where

$$\mathbf{n} = -\frac{\mathbf{X}}{\|\mathbf{X}\|} \times (1, 0, 0), \quad \cos(\theta) = -\frac{X^1}{\|\mathbf{X}\|}, \quad (\text{C.15})$$

and  $\mathbf{L} = (L_x, L_y, L_z)$  are the infinitesimal rotations along the three axes (as  $4 \times 4$  anti-symmetric matrices). Next we need a boost  $B \in SO(3, 1) \subset \mathbb{P}$ , in the  $x$ -direction and parametrized by  $w$

$$B \cdot \begin{pmatrix} t \\ x \\ y \\ z \end{pmatrix} = \begin{pmatrix} \gamma(t - xw) \\ \gamma(x - tw) \\ y \\ z \end{pmatrix} \quad (\text{C.16})$$

in order to eliminate the remaining non-zero spatial component. The transformation leads to

$$BR(P - X) = \gamma \begin{pmatrix} -X^0 - \|\mathbf{X}\|w \\ \|\mathbf{X}\| + X^0w \\ 0 \\ 0 \end{pmatrix}. \quad (\text{C.17})$$

We choose the velocity  $w$  such that the spatial component vanishes

$$w = -\frac{\|\mathbf{X}\|}{X^0}. \quad (\text{C.18})$$

Thus finally the coordinate  $P$  is mapped to

$$\tilde{P} = BR(P - X) = \left( \tilde{P}^0, \mathbf{0} \right)_{\tilde{Y}}, \quad (\text{C.19})$$

where

$$\tilde{P}^0 = \gamma \left( -X^0 + \frac{\|\mathbf{X}\|^2}{X^0} \right). \quad (\text{C.20})$$

The coordinate transformation is thus

$$\tilde{Y} = BR(Y - X). \quad (\text{C.21})$$

In this coordinate system the region  $\mathcal{J}^-(x) = I(x, p)$  will look like a standard upright diamond between the points  $\tilde{P} = (\tilde{P}^0, \mathbf{0})_{\tilde{Y}}$  and  $\tilde{X} = (0, \mathbf{0})_{\tilde{Y}}$ . We will now parametrize  $\mathcal{J}^-(x)$  using radial lightcone coordinates. First we use spherical coordinates  $(\tilde{Y}^0, \tilde{Y}^1, \tilde{Y}^2, \tilde{Y}^3) \rightarrow (\tilde{Y}^0, r, \theta, \phi)$  where

$$\begin{aligned} \tilde{Y}^1 &= r \cos \theta, \\ \tilde{Y}^2 &= r \cos \phi \sin \theta, \\ \tilde{Y}^3 &= r \sin \phi \sin \theta. \end{aligned} \quad (\text{C.22})$$

In particular,  $r = \|\tilde{\mathbf{Y}}\|$ . Then we use the radial lightcone coordinates  $(\tilde{Y}^0, r, \theta, \phi) \rightarrow (u, v, \theta, \phi)$

$$\begin{aligned} u &= \frac{1}{\sqrt{2}} \left( \tilde{Y}^0 - \|\tilde{\mathbf{Y}}\| \right), \\ v &= \frac{1}{\sqrt{2}} \left( \tilde{Y}^0 + \|\tilde{\mathbf{Y}}\| \right). \end{aligned} \quad (\text{C.23})$$

The combined coordinate transformation is thus

$$\begin{aligned} \tilde{Y}^0 &= \frac{(v+u)}{\sqrt{2}}, & \tilde{Y}^2 &= \frac{(v-u)}{\sqrt{2}} \cos \phi \sin \theta, \\ \tilde{Y}^1 &= \frac{(v-u)}{\sqrt{2}} \cos \theta, & \tilde{Y}^3 &= \frac{(v-u)}{\sqrt{2}} \sin \phi \sin \theta. \end{aligned} \quad (\text{C.24})$$

The volume form is given by

$$\begin{aligned} d^4y &= dY^0 dY^1 dY^2 dY^3 \\ &= d\tilde{Y}^0 d\tilde{Y}^1 d\tilde{Y}^2 d\tilde{Y}^3, \\ &= r^2 d\tilde{Y}^0 dr d^2\Omega, \\ &= \frac{1}{2} (v-u)^2 du dv d^2\Omega. \end{aligned} \quad (\text{C.25})$$

$$\mathcal{J}^-(x) = \left\{ (u, v, \theta, \phi) \mid u \in \left[ 0, -\frac{1}{\sqrt{2}}\tau_{px} \right] \wedge v \in [0, u] \wedge \theta \in [0, \pi] \wedge \phi \in [0, 2\pi] \right\}, \quad (\text{C.26})$$

where  $\tau_{px} = \tilde{P}^0$ . The mapping  $Y = R^{-1}B^{-1}\tilde{Y} + X$  together with equations (C.24), allows us to express  $Y = Y(u, v, \theta, \phi)$ . In particular, we can compute the integrals over  $\mathcal{J}^-(x)$  as

$$\int_{\mathcal{J}^-(x)} f(Y) d^4Y = \int_{S^2} d^2\Omega \int_0^{-\frac{\tau_{px}}{\sqrt{2}}} du \int_0^u dv \frac{1}{2}(v-u)^2 f(Y(u, v, \theta, \phi)) \quad (\text{C.27})$$

## Acknowledgments

We acknowledge the support of the European Consortium for Astroparticle Theory (EuCAPT) in the form of an Exchange Travel Grant held at CERN. HM is supported by the Leverhulme Trust Early Career Fellowship. YY acknowledges financial support from Research Ireland under Grant number 22/PATH-S/10704, as well as support from a Leverhulme Trust Research Project Grant. MZ acknowledges financial support by the Center for Research and Development in Mathematics and Applications (CIDMA) through the Portuguese Foundation for Science and Technology (FCT – Fundação para a Ciência e a Tecnologia) through projects: UIDB/04106/2020 (with DOI identifier <https://doi.org/10.54499/UIDB/04106/2020>); UIDP/04106/2020 (DOI identifier <https://doi.org/10.54499/UIDP/04106/2020>); PTDC/FIS-AST/3041/2020 (DOI identifier <http://doi.org/10.54499/PTDC/FIS-AST/3041/2020>); CERN/FIS-PAR/0024/2021 (DOI identifier <http://doi.org/10.54499/CERN/FIS-PAR/0024/2021>); 2022.04560.PTDC (DOI identifier <https://doi.org/10.54499/2022.04560.PTDC>); and 2022.00721.CEECIND (DOI identifier <https://doi.org/10.54499/2022.00721.CEECIND/CP1720/CT0001>).

## References

- [1] L. Bombelli, J. Lee, D. Meyer and R.D. Sorkin, *Space-time as a causal set*, *Phys. Rev. Lett.* **59** (1987) 521.
- [2] S. Surya, *The causal set approach to quantum gravity*, *Living Rev. Rel.* **22** (2019) 5 [[1903.11544](https://arxiv.org/abs/1903.11544)].
- [3] R.D. Sorkin, *Ten theses on black hole entropy*, *Stud. Hist. Phil. Sci. B* **36** (2005) 291 [[hep-th/0504037](https://arxiv.org/abs/hep-th/0504037)].
- [4] H.B. Nielsen and M. Ninomiya, *The Adler-Bell-Jackiw anomaly and Weyl fermions in a crystal*, *Phys. Lett. B* **130** (1983) 389.
- [5] H.B. Nielsen and M. Ninomiya, *Absence of Neutrinos on a Lattice. 1. Proof by Homotopy Theory*, *Nucl. Phys. B* **185** (1981) 20.
- [6] H.B. Nielsen and M. Ninomiya, *Absence of Neutrinos on a Lattice. 2. Intuitive Topological Proof*, *Nucl. Phys. B* **193** (1981) 173.
- [7] H.B. Nielsen and M. Ninomiya, *No Go Theorem for Regularizing Chiral Fermions*, *Phys. Lett. B* **105** (1981) 219.
- [8] S.M. Kravec and J. McGreevy, *A gauge theory generalization of the fermion-doubling theorem*, *Phys. Rev. Lett.* **111** (2013) 161603 [[1306.3992](https://arxiv.org/abs/1306.3992)].

- [9] M. Saravani and S. Aslanbeigi, *On the Causal Set-Continuum Correspondence*, *Class. Quant. Grav.* **31** (2014) 205013 [[1403.6429](#)].
- [10] J. Henson, D.P. Rideout, R.D. Sorkin and S. Surya, *Onset of the Asymptotic Regime for Finite Orders*, [1504.05902](#).
- [11] S. Carlip, *Causal sets and an emerging continuum*, *Gen. Rel. Grav.* **56** (2024) 95 [[2405.14059](#)].
- [12] S. Johnston, *Feynman Propagator for a Free Scalar Field on a Causal Set*, *Phys. Rev. Lett.* **103** (2009) 180401 [[0909.0944](#)].
- [13] N. X., *Quantum Field Theory on Causal Sets*, (2024), DOI [[2306.04800](#)].
- [14] E. Albertini, F. Dowker, A. Nasiri and S. Zalel, *In-in correlators and scattering amplitudes on a causal set*, *Phys. Rev. D* **109** (2024) 106014 [[2402.08555](#)].
- [15] R.D. Sorkin, *Expressing entropy globally in terms of (4D) field-correlations*, *J. Phys. Conf. Ser.* **484** (2014) 012004 [[1205.2953](#)].
- [16] Y.K. Yazdi, *Entanglement Entropy and Causal Set Theory*, [2212.13586](#).
- [17] V. Homšak and S. Veroni, *Boltzmannian state counting for black hole entropy in causal set theory*, *Phys. Rev. D* **110** (2024) 026015 [[2404.11670](#)].
- [18] R.D. Sorkin, *Does locality fail at intermediate length-scales*, [gr-qc/0703099](#).
- [19] D.M.T. Benincasa and F. Dowker, *Scalar curvature of a causal set*, *Physical Review Letters* **104** (2010) [[1001.2725](#)].
- [20] R.D. Sorkin, *A Modified Sum-Over-Histories for Gravity reported in the article by D. Brill and L. Smolin: “Workshop on quantum gravity and new directions”*, in *Highlights in gravitation and cosmology: Proceedings of the International Conference on Gravitation and Cosmology, Goa, India, 14–19 December 1987*, B.R. Iyer, A. Kembhavi, J.V. Narlikar and C.V. Vishveshwara, eds., pp. 184–186, 1988.
- [21] R.D. Sorkin, *Role of time in the sum-over-histories framework for gravity*, *International journal of theoretical physics* **33** (1994) 523.
- [22] M. Ahmed, S. Dodelson, P.B. Greene and R. Sorkin, *Everpresent  $\Lambda$* , *Physical Review D* **69** (2004) 103523 [[astro-ph/0209274](#)].
- [23] S. Das, A. Nasiri and Y.K. Yazdi, *Aspects of Everpresent  $\Lambda$ . Part I. A fluctuating cosmological constant from spacetime discreteness*, *JCAP* **10** (2023) 047 [[2304.03819](#)].
- [24] Y.K. Yazdi, *Everything you always wanted to know about how causal set theory can help with open questions in cosmology, but were afraid to ask*, *Mod. Phys. Lett. A* **39** (2024) 2330003 [[2311.14881](#)].
- [25] E. Abdalla et al., *Cosmology intertwined: A review of the particle physics, astrophysics, and cosmology associated with the cosmological tensions and anomalies*, *JHEAp* **34** (2022) 49 [[2203.06142](#)].
- [26] L. Perivolaropoulos and F. Skara, *Challenges for  $\Lambda$ CDM: An update*, *New Astron. Rev.* **95** (2022) 101659 [[2105.05208](#)].
- [27] S. Vagnozzi, *Seven Hints That Early-Time New Physics Alone Is Not Sufficient to Solve the Hubble Tension*, *Universe* **9** (2023) 393 [[2308.16628](#)].

- [28] E. Di Valentino, O. Mena, S. Pan, L. Visinelli, W. Yang, A. Melchiorri et al., *In the realm of the Hubble tension—a review of solutions*, *Class. Quant. Grav.* **38** (2021) 153001 [[2103.01183](#)].
- [29] DESI collaboration, *DESI 2024 VI: Cosmological Constraints from the Measurements of Baryon Acoustic Oscillations*, [2404.03002](#).
- [30] R.D. Sorkin, *Causal sets: Discrete gravity*, in *School on Quantum Gravity*, pp. 305–327, 9, 2003, DOI [[gr-qc/0309009](#)].
- [31] F. Dowker and J. Butterfield, *Recovering General Relativity from a Planck scale discrete theory of quantum gravity*, [2106.01297](#).
- [32] S.P. Loomis and S. Carlip, *Suppression of non-manifold-like sets in the causal set path integral*, *Class. Quant. Grav.* **35** (2018) 024002 [[1709.00064](#)].
- [33] P. Carlip, S. Carlip and S. Surya, *Path integral suppression of badly behaved causal sets*, *Class. Quant. Grav.* **40** (2023) 095004 [[2209.00327](#)].
- [34] P. Carlip, S. Carlip and S. Surya, *The Einstein-Hilbert Action for Entropically Dominant Causal Sets*, [2311.18238](#).
- [35] A. Papoulis and S. Pillai, *Probability, Random Variables, and Stochastic Processes*, McGraw-Hill series in electrical engineering: Communications and signal processing, Tata McGraw-Hill (2002).
- [36] V. Petrov, *Limit Theorems of Probability Theory: Sequences of Independent Random Variables*, Oxford science publications, Clarendon Press (1995).
- [37] J. Kingman, *Poisson Processes*, Oxford science publications, Clarendon Press (1993).
- [38] E. Wigner and F. Seitz, *On the constitution of metallic sodium*, *Phys. Rev.* **43** (1933) 804.
- [39] F. Dowker, J. Henson and R. Sorkin, *Discreteness and the transmission of light from distant sources*, *Phys. Rev. D* **82** (2010) 104048 [[1009.3058](#)].
- [40] F. Dowker and L. Glaser, *Causal set d’alembertians for various dimensions*, *Classical and Quantum Gravity* **30** (2013) 195016 [[1305.2588](#)].
- [41] L. Glaser, *A closed form expression for the causal set d’Alembertian*, *Class. Quant. Grav.* **31** (2014) 095007 [[1311.1701](#)].
- [42] K. Yeats, *Combinatorial interpretation of the coefficients of the causal set d’Alembertian*, [2412.14036](#).
- [43] A. Nasiri, *Synge’s world function applied to causal diamonds and causal sets*, [2304.00088](#).
- [44] G.P. de Brito, A. Eichhorn and C. Pfeiffer, *Higher-order curvature operators in causal set quantum gravity*, *Eur. Phys. J. Plus* **138** (2023) 592 [[2301.13525](#)].
- [45] D.M.T. Benincasa, *The Action of a Causal Set*, Ph.D. thesis, 2013.
- [46] S. Aslanbeigi, M. Saravani and R.D. Sorkin, *Generalized causal set d’Alembertians*, *JHEP* **06** (2014) 024 [[1403.1622](#)].
- [47] A. Belenchia, D.M.T. Benincasa and F. Dowker, *The continuum limit of a 4-dimensional causal set scalar d’Alembertian*, *Class. Quant. Grav.* **33** (2016) 245018 [[1510.04656](#)].
- [48] S. Das, A. Nasiri and Y.K. Yazdi, *Aspects of Everpresent  $\Lambda$  (II): Cosmological Tests of Current Models*, [2307.13743](#).



- [49] F. Dowker, *Boundary contributions in the causal set action*, *Gen. Rel. Grav.* **38** (2021) 075018 [[2007.13206](#)].
- [50] L. Machet and J. Wang, *On the continuum limit of benincasa–dowker–glaser causal set action*, *Classical and Quantum Gravity* **38** (2020) 015010 [[2007.13192](#)].